Cold Dark Matter and Higgs Mass in the Constrained Minimal Supersymmetric Standard Model with Generalized Yukawa Quasi-Unification

N. Karagiannakis

Physics Division, School of Technology, Aristotle University of Thessaloniki, 54124 Thessaloniki, GREECE nikar@auth.gr

G. Lazarides

Physics Division, School of Technology, Aristotle University of Thessaloniki, 54124 Thessaloniki, GREECE lazaride@eng.auth.gr

C. Pallis

Department of Physics, University of Cyprus, P.O. Box 20537, CY-1678 Nicosia, CYPRUS cpallis@ucy.ac.cy

The construction of specific supersymmetric grand unified models based on the Pati-Salam gauge group and leading to a set of Yukawa quasi-unification conditions which can allow an acceptable b-quark mass within the constrained minimal supersymmetric standard model with $\mu>0$ is briefly reviewed. Imposing constraints from the cold dark matter abundance in the universe, B physics, and the mass m_h of the lighter neutral CP-even Higgs boson, we find that there is an allowed parameter space with, approximately, $44 \le \tan \beta \le 52$, $-3 \le A_0/M_{1/2} \le 0.1$, $122 \le m_h/\text{GeV} \le 127$, and mass of the lightest sparticle in the range (0.75-1.43) TeV. Such heavy lightest sparticle masses can become consistent with the cold dark matter requirements on the lightest sparticle relic density thanks to neutralino-stau coannihilations which are enhanced due to stau-antistau coannihilation to down type fermions via a direct-channel exchange of the heavier neutral CP-even Higgs boson. Restrictions on the model parameters by the muon anomalous magnetic moment are also discussed.

Keywords: Supersymmetry; Dark Matter; Higgs Mass.

PACS numbers: 12.10.Kt, 12.60.Jv, 95.35.+d

1. Prologue

The constrained minimal supersymmetric standard model (CMSSM) is a highly predictive version of the minimal supersymmetric standard model (MSSM) based on universal boundary conditions. ^{1–9} It can be further restricted by being embedded in a supersymmetric (SUSY) grand unified theory (GUT) with a gauge group containing $SU(4)_c$ and $SU(2)_R$. This can lead ^{10,11} to 'asymptotic' Yukawa unification (YU), ^{12,13} i.e. the exact unification of the third generation Yukawa coupling constants at the supersymmetric (SUSY)

GUT scale $M_{\rm GUT}$. In this scheme, we take the electroweak Higgs superfields H_1 , H_2 and the third family right handed quark superfields t^c , b^c to form $SU(2)_R$ doublets. As a result, we obtain 10,11 the asymptotic Yukawa coupling relation $h_t=h_b$ and, hence, large $\tan \beta \sim m_t/m_b$. Furthermore, to get $h_b=h_\tau$ and, thus, the asymptotic relation $m_b=m_\tau$, the third generation quark and lepton $SU(2)_L$ doublets [singlets] q_3 and l_3 [b^c and τ^c] have to form a $SU(4)_c$ 4-plet [$\bar{4}$ -plet], while the Higgs doublet H_1 which couples to them has to be a $SU(4)_c$ singlet. The simplest GUT gauge group which contains both $SU(4)_c$ and $SU(2)_R$ is the Pati-Salam (PS) group $G_{\rm PS}=SU(4)_c\times SU(2)_L\times SU(2)_R$ – for YU within SO(10), see Ref. 14–16.

Given the experimental values of the top-quark and tau-lepton masses, the CMSSM supplemented by the assumption of YU (which naturally restricts $\tan \beta \sim 50$) yields unacceptable values of the b-quark mass for both signs of the MSSM parameter μ . Moreover, the generation of sizable SUSY corrections $^{17-19}$ to m_b (about 20%) drive it well beyond the experimentally allowed region with the $\mu < 0$ case being much less disfavored. Despite this fact, we prefer to focus on the $\mu > 0$ case, since $\mu < 0$ is strongly disfavored by the constraint arising from the deviation δa_μ of the measured value of the muon anomalous magnetic moment a_μ from its predicted value $a_\mu^{\rm SM}$ in the standard model (SM). Indeed, $\mu < 0$ is defended only at $3 - \sigma$ by the calculation of $a_\mu^{\rm SM}$ based on the τ -decay data, whereas there is a stronger and stronger tendency at present to prefer the e^+e^- annihilation data for the calculation of $a_\mu^{\rm SM}$, which favor the $\mu > 0$ regime. Note that, the results of Ref. 23,24, where it is claimed that the mismatch between the τ - and e^+e^- -based calculations is alleviated, disfavor $\mu < 0$ even more strongly.

The usual strategy to solve the aforementioned tension between exact YU and fermion masses is the introduction of several kinds of nonuniversalities in the scalar ^{14–16,25–31} and/or gaugino ^{32–34} sector of MSSM with an approximate preservation of YU. On the contrary, in Ref. 35 – see also Refs. 36–42 –, this problem is addressed in the context of the PS GUT model, without the need of invoking departure from the CMSSM universality. We prefer to sacrifice the exact YU in favor of the universality hypothesis, since we consider this hypothesis as more economical, predictive, and easily accommodated within conventional SUSY GUT models. Indeed, it is known – cf. first paper in Ref. 43–46 – that possible violation of universality, which could arise from D-term contributions if the MSSM is embedded into the PS GUT model, does not occur provided that the soft SUSY breaking scalar masses of the superheavy fields which break the GUT gauge symmetry are assumed to be universal.

In the proposal of Ref. 35, the Higgs sector of the simplest PS model^{47,48} is extended by including an extra $SU(4)_{\rm c}$ nonsinglet Higgs superfield with Yukawa couplings to the quarks and leptons. The Higgs $SU(2)_L$ doublets in this superfield can naturally develop^{49,50} subdominant vacuum expectation values (VEVs) and mix with the main electroweak doublets, which are $SU(4)_{\rm c}$ singlets and form a $SU(2)_R$ doublet. The resulting electroweak doublets H_1, H_2 break $SU(4)_{\rm c}$ and do not form a $SU(2)_R$ doublet. Thus, YU is replaced by a set of Yukawa quasi-unification conditions (YQUCs) which depend on up to five extra real parameters. The number of these parameters depends on the representations used for the Higgs superfields which mix the $SU(2)_L$ doublets in the $SU(4)_{\rm c}$ singlet and

nonsinglet Higgs bidoublets and some simplifying assumptions. These Higgs superfields can either belong to a triplet or a singlet representation of $SU(2)_R$. In the past, ^{35–38} we have shown that the monoparametric YQUCs emerging from the inclusion of one $SU(2)_R$ triplet [singlet] superfield could give a SUSY model with correct fermion masses for $\mu > 0$ $[\mu < 0]$. However, only the model with $\mu > 0$ could survive^{37–39,41,42} after imposing a set of cosmological and phenomenological constraints. The same model can also support new successful versions^{51–55} of hybrid inflation, based solely on renormalizable superpotential terms and avoiding overproduction of monopoles. 56-59 The baryon asymmetry of the universe may be generated via nonthermal leptogenesis. 60,61

However, the recently announced data - most notably by the Large Hadron Collider (LHC) - on the mass of the SM-like Higgs boson⁶²⁻⁶⁴ as well as the branching ratio BR $(B_s \to \mu^+ \mu^-)$ of the process $B_s \to \mu^+ \mu^{-65,66}$ in conjunction with cold dark matter (CDM) considerations⁶⁷ destroyed the successful picture above. To be more specific, the upper bound from CDM considerations on the lightest neutralino relic density, which is strongly reduced by neutralino-stau coannihilations, yields a very stringent upper bound on the mass of the lightest neutralino $m_{\tilde{\chi}}$, which is incompatible with the lower bound on $m_{\tilde{\chi}}$ from the data^{65,66,68} on BR $(B_s \to \mu^+ \mu^-)$. The main reason for this negative result is that $\tan \beta$ remains large and, thus – see Sec. 4 –, the SUSY contribution to BR $(B_s \to \mu^+ \mu^-)$ turns out to be too large. To overcome this hurdle, we included in Ref. 69 both $SU(2)_R$ -triplet and singlet Higgs superfields. This allows for a more general version of the YQUCs, which now depend on one real and two complex parameters. As a consequence, the third generation Yukawa coupling constants are freed from the stringent constraint $h_b/h_t + h_\tau/h_t = 2$ obtained in the monoparametric case and, thus, we can accommodate more general values of the ratios h_m/h_n with $m, n = t, b, \tau$, which are expected, of course, to be of order unity for natural values of the model parameters. Moreover, lower $\tan \beta$'s are allowed reducing thereby the extracted BR $(B_s \to \mu^+ \mu^-)$ to a level compatible with the CDM requirement. The allowed parameter space of the model is then mainly determined by the interplay of the constraints from BR $(B_s \to \mu^+\mu^-)$ and CDM and the recently announced results of LHC on the Higgs boson mass m_h .

In this review, we outline the construction of the SUSY GUT model which can cause an adequate deviation from exact YU with sufficiently low $\tan \beta$ so as the resulting CMSSM with $\mu > 0$ to be consistent with a number of astrophysical and experimental requirements. They originate most notably from the data on m_h and the BR $(B_s \to \mu^+ \mu^-)$ derived by LHC and the nine-year fitting of the observations of the Wilkinson microwave anisotropy probe (WMAP)⁶⁷ on the CDM abundance. We show that the allowed parameter space of the model is relatively wide, but the sparticle masses are too heavy lying in the multi-TeV range. The latter signalizes a mild amount of tuning as regards the achievement of the electroweak symmetry breaking (EWSB).

The construction of the model is briefly reviewed in Sec. 2 and the resulting CMSSM is presented in Sec. 3. The parameter space of the CMSSM is restricted in Sec. 6 taking into account a number of phenomenological and cosmological requirements, which are exhibited in Secs. 4 and 5 respectively. The deviation from exact YU is estimated in Sec. 7. Finally, we summarize our conclusions in Sec. 9.

2. The Pati-Salam Supersymmetric GUT Model

We outline below – in Sec. 2.1 – the salient features of our model and then analyze the various parts of its superpotential in Secs. 2.2, 2.3, 2.4, and 2.5. Finally, we discuss the issue of the stability of the proton in Sec. 2.6.

2.1. The General Set-up

We focus on the SUSY PS GUT model which is described in detail in Ref. 48 – see also Refs. 37, 38, 70. The representations and the transformation properties under $G_{\rm PS}$ of the various matter and Higgs superfields contained in the model as well as their extra global charges (see below) are included in Table 1. The ith generation (i=1,2,3) left handed (LH) quark [lepton] superfields u_{ia} and d_{ia} – where a=1,2,3 is a color index – [e_i and ν_i] are accommodated in the superfields F_i . The LH antiquark [antilepton] superfields u_{ia}^c and d_{ia}^c [e_i^c and ν_i^c] are arranged in the superfields F_i^c . These superfields can be represented as

$$F_{i} = \left(q_{i1} \ q_{i2} \ q_{i3} \ l_{i}\right) \text{ and } F_{i}^{c} = \begin{pmatrix} q_{i1}^{c} \\ q_{i2}^{c} \\ q_{i3}^{c} \\ l_{i}^{c} \end{pmatrix} \text{ with }$$

$$q_{ia} = \left(d_{ia} - u_{ia}\right), \ l_{i} = \left(e_{i} - \nu_{i}\right), \ q_{ia}^{c} = \begin{pmatrix} -u_{ia}^{c} \\ d_{ia}^{c} \end{pmatrix}, \ l_{i}^{c} = \begin{pmatrix} -\nu_{i}^{c} \\ e_{i}^{c} \end{pmatrix}. \tag{1}$$

The gauge symmetry $G_{\rm PS}$ can be spontaneously broken down to the SM gauge group $G_{\rm SM}$ through the VEVs which the superfields

$$H^{c} = \begin{pmatrix} q_{H1}^{c} \\ q_{H2}^{c} \\ q_{H3}^{c} \\ l_{H}^{c} \end{pmatrix} \text{ and } \bar{H}^{c} = \begin{pmatrix} \bar{q}_{H1}^{c} \bar{q}_{H2}^{c} \bar{q}_{H3}^{c} \bar{l}_{H}^{c} \end{pmatrix} \text{ with }$$

$$q_{Ha}^{c} = \begin{pmatrix} u_{Ha}^{c} \\ d_{Ha}^{c} \end{pmatrix}, l_{H}^{c} = \begin{pmatrix} \nu_{H}^{c} \\ e_{H}^{c} \end{pmatrix}, \bar{q}_{Ha}^{c} = \begin{pmatrix} \bar{u}_{Ha}^{c} \bar{d}_{Ha}^{c} \end{pmatrix}, \bar{l}_{H}^{c} = \begin{pmatrix} \bar{\nu}_{H}^{c} \bar{e}_{H}^{c} \end{pmatrix}$$
(2)

acquire in the direction ν_H^c and $\bar{\nu}_H^c$, respectively. The model also contains a gauge singlet S, which triggers the breaking of $G_{\rm PS}$, as well as a $SU(4)_c$ **6**-plet G, which splits under G_{SM} into a $SU(3)_c$ triplet $g_{\rm a}^c$ and antitriplet $\bar{g}_{\rm a}^c$, which give⁴⁷ superheavy masses to d_{Ha}^c and \bar{d}_{Ha}^c . In particular, G can be represented by an antisymmetric 4×4 matrix

$$G = \begin{pmatrix} \varepsilon_{\text{abc}} g_{\text{c}}^c \bar{g}_{\text{a}}^c \\ -\bar{g}_{\text{a}}^c & 0 \end{pmatrix} \Rightarrow \bar{G} = \begin{pmatrix} \varepsilon_{\text{abc}} \bar{g}_{\text{c}}^c g_{\text{a}}^c \\ -g_{\text{a}}^c & 0 \end{pmatrix}, \tag{3}$$

where \bar{G} is the dual tensor of G defined by $\bar{G}_{IJ} = \varepsilon_{IJKL}G_{KL}$ and transforms under $SU(4)_c$ as $U_c^*\bar{G}U_c^{\dagger}$. Here, ε_{IJKL} [ε_{abc}] is the well-known antisymmetric tensor acting on the $SU(4)_c$ [$SU(3)_c$] indices with $\varepsilon_{1234} = 1$ [$\varepsilon_{123} = 1$]. The symmetries of the model allow the presence of quartic (nonrenormalizable) superpotential couplings of \bar{H}^c to

Table 1. The representations and transformations under G_{PS} as well as the extra global charges of the superfields of our model $(U_{\rm c} \in SU(4)_{\rm c},\ U_L \in SU(2)_L,\ U_R \in SU(2)_R$ and T ,†, and * stand for the transpose, the hermitian conjugate, and the complex conjugate of a matrix respectively).

Super- fields	Representations under G_{PS}	Trasformations under G_{PS}	R	$\mathbb{Z}_2^{\mathrm{mp}}$				
Matter Superfields								
$F_i \\ F_i^c$	$egin{array}{c} ({f 4},{f 2},{f 1}) \ ({f ar 4},{f 1},{f 2}) \end{array}$	$F_i U_L^{\dagger} U_c^{T} \\ U_c^* U_R^* F_i^c$	1/2 $1/2$	-1 0	1 -1			
Higgs Superfields								
H^c \bar{H}^c S G	$egin{array}{c} (ar{4},1,2) \\ (4,1,2) \\ (1,1,1) \\ (6,1,1) \end{array}$	$U_{\mathbf{c}}^{*}U_{R}^{*}H^{c}$ $\bar{H}^{c}U_{R}^{T}U_{\mathbf{c}}^{T}$ S $U_{\mathbf{c}}GU_{\mathbf{c}}^{T}$	0 0 1 1	0 0 0	0 0 0 0			
h	$({f 1},{f 2},{f 2})$	$U_L I h U_R^{T}$	0	1	0			
$N \over ar{N}$	$({f 1},{f 1},{f 1}) \ ({f 1},{f 1},{f 1})$	$N \over ar{N}$	$_{0}^{1/2}$	-1 1	0			
Extra Higgs Superfields								
<i>l</i> h′ <i>l</i> h′	$({f 15},{f 2},{f 2}) \ ({f 15},{f 2},{f 2})$	$\begin{array}{c} U_{\mathrm{c}}^{*}U_{L} \!\!\!\! \! \! \! \! \! \! \! \! \! \! \! \! \! \! \! \! $	0 1	1 -1	0			
$rac{\phi}{ar{\phi}}$	$({f 15},{f 1},{f 3}) \ ({f 15},{f 1},{f 3})$	$U_{\rm c}U_R\phi U_R^{\dagger}U_{\rm c}^{\dagger}$ $U_{\rm c}U_R\bar{\phi}U_R^{\dagger}U_{\rm c}^{\dagger}$	0 1	0 0	0			
$\frac{\phi'}{\bar{\phi}'}$	(15, 1, 1) (15, 1, 1)	$U_{ m c}\phi'U_{ m c}^{\dagger} \ U_{ m c}ar{\phi}'U_{ m c}^{\dagger}$	0 1	0	0			

 F_i^c , which generate intermediate-scale masses for the right handed neutrinos ν_i^c and, thus, masses for the light neutrinos ν_i via the seesaw mechanism.

In addition to G_{PS} , the model possesses two global U(1) symmetries, namely a Peccei-Quinn (PQ)⁷¹⁻⁷³ and a R symmetry, as well as a discrete $Z_2^{\rm mp}$ symmetry ('matter parity') under which F, F^c change sign. Note that global continuous symmetries such as our PQ and R symmetry can effectively arise⁷⁴ from the rich discrete symmetry groups encountered in many compactified string theories – see e.g. Ref. 75, 76.

In the simplest realization of this model, 37,38,47 the electroweak doublets H_1, H_2 are exclusively contained in the bidoublet superfield Ih, which can be written as

$$Ih = \left(Ih_2 Ih_1\right), \tag{4}$$

and so the model predicts YU at $M_{\rm GUT}$ – note that $M_{\rm GUT}$ is determined by the requirement of the unification of the gauge coupling constants. In order to allow for a sizable violation of YU, we extend the model by including three extra pairs of Higgs superfields $I\!h', \bar{I}\!h', \phi, \bar{\phi}$, and $\phi', \bar{\phi}'$, where the barred superfields are included in order to give superheavy masses to the unbarred superfields. These extra Higgs superfields together with their transformation properties and charges under the global symmetries of the model are also included in Table 1. The two new Higgs superfields $I\!h'$ and $\bar{I}\!h'$ with

$$Ih' = \left(Ih'_2 Ih'_1 \right) \text{ and } \bar{Ih}' = \left(\bar{I}h'_2 \bar{I}h'_1 \right)$$
 (5)

belong to the (15,2,2) representation of $SU(4)_c$, which is the only representation besides (1,2,2) that can couple to the fermions. On the other hand, ϕ and ϕ' acquire superheavy VEVs of order $M_{\rm GUT}$ after the breaking of $G_{\rm PS}$ to $G_{\rm SM}$. Their couplings with $\bar{I}\!\!h'$ and $I\!\!h$ naturally generate a $SU(2)_R$ - and $SU(4)_c$ -violating mixing of the $SU(2)_L$ doublets in $I\!\!h$ and $I\!\!h'$ leading, thereby, to a sizable violation of YU.

More explicitly, the superpotential W of our model naturally splits into four parts

$$W = W_{\rm H} + W_{\rm M} + W_{\rm Y} + W_{\rm PO},$$
 (6)

which are specified, in turn, in the following Secs. 2.2, 2.3, 2.4, and 2.5.

2.2. The Spontaneous Breaking of G_{PS} to G_{SM}

The part of W in Eq. (6) which is relevant for the breaking of G_{PS} to G_{SM} is given by

$$W_{\rm H} = \kappa S \left(H^c \bar{H}^c - M^2 \right) - S \left(\beta \phi^2 + \beta' \phi'^2 \right) + \left(\lambda \bar{\phi} + \lambda' \bar{\phi}' \right) H^c \bar{H}^c + m \phi \bar{\phi} + m' \phi' \bar{\phi}', \tag{7}$$

where the mass parameters M, m, and m' are of order $M_{\rm GUT}$ and κ , β , β' , λ , and λ' are dimensionless complex parameters. Note that by field redefitions we can set M, m, m', κ , λ , and λ' to be real and positive. For simplicity, we also take $\beta > 0$ and $\beta' > 0$ (the parameters are normalized so that they correspond to the couplings between the SM singlet components of the superfields).

The scalar potential obtained from $W_{\rm H}$ is given by

$$V_{H} = \left| \kappa (H^{c} \bar{H}^{c} - M^{2}) - \beta \phi^{2} - \beta' \phi'^{2} \right|^{2} + \left| \kappa S + \lambda \bar{\phi} + \lambda' \bar{\phi}' \right|^{2} \left(|H^{c}|^{2} + |\bar{H}^{c}|^{2} \right)$$

$$+ \left| m \phi + \lambda H^{c} \bar{H}^{c} \right|^{2} + \left| m' \phi' + \lambda' H^{c} \bar{H}^{c} \right|^{2}$$

$$+ \left| 2\beta S \phi - m \bar{\phi} \right|^{2} + \left| 2\beta' S \phi' - m' \bar{\phi}' \right|^{2} + D - \text{terms},$$
(8)

where the complex scalar fields which belong to the SM singlet components of the superfields are denoted by the same symbols as the corresponding superfields. Vanishing of the D-terms yields $\bar{H}^{c\,*}=e^{i\vartheta}H^c$ (H^c , \bar{H}^c lie in the ν_H^c , $\bar{\nu}_H^c$ direction). We restrict ourselves to the direction with $\vartheta=0$, which contains the SUSY vacua (see below). Performing appropriate R and gauge transformations, we bring H^c , \bar{H}^c , and S to the positive real axis.

From the potential in Eq. (8), we find that the SUSY vacuum lies at

$$\langle H^c \bar{H}^c \rangle = v_0^2, \ \langle S \rangle = \langle \bar{\phi} \rangle = \langle \bar{\phi}' \rangle = 0$$
 (9a)

and

$$\langle \phi \rangle = v_{\phi} \left(T_{c}^{15}, 1, \frac{\sigma_{3}}{\sqrt{2}} \right), \ \langle \phi' \rangle = v_{\phi}' \left(T_{c}^{15}, 1, \frac{\sigma_{0}}{\sqrt{2}} \right),$$
 (9b)

where

$$\left(\frac{v_0}{M}\right)^2 = \frac{1}{2\xi} \left(1 - \sqrt{1 - 4\xi}\right), \ v_\phi = -\lambda \frac{v_0^2}{m}, \ v_\phi' = -\lambda' \frac{v_0^2}{m'}$$
(9c)

with

$$\xi = \frac{M^2}{\kappa} \left(\frac{\beta \lambda^2}{m^2} + \frac{\beta' \lambda'^2}{m'^2} \right) < 1/4. \tag{9d}$$

The structure of $\langle \phi \rangle$ and $\langle \phi' \rangle$ with respect to (w.r.t.) $G_{\rm PS}$ is shown in Eq. (9b), where

$$T_{\rm c}^{15} = \frac{1}{2\sqrt{3}} \, {\rm diag} \left(1, 1, 1, -3\right), \ \sigma_3 = {\rm diag} \left(1, -1\right), \ {\rm and} \ \sigma_0 = {\rm diag} \left(1, 1\right).$$
 (10a)

2.3. Mass Terms

The part of W in Eq. (6) which gives masses to the various components of the superfields naturally splits into three parts

$$W_{\rm M} = W_G + W_{\rm RHN} + W_{\rm mix} \tag{11}$$

out of which the first one is responsible for the generation of superheavy masses for the superfields d_H^c and \bar{d}_H^c :

$$W_{G} = \lambda_{H} H^{c\mathsf{T}} G \varepsilon H^{c} + \lambda_{\bar{H}} \bar{H}^{c} \bar{G} \varepsilon \bar{H}^{c\mathsf{T}}$$

$$= -2\lambda_{H} \left(\nu_{H}^{c} d_{H}^{c} - e_{H}^{c} u_{H}^{c} \right) \bar{g}^{c} + 2\lambda_{H} u_{H}^{c} d_{H}^{c} g^{c}$$

$$-2\lambda_{\bar{H}} \left(\bar{\nu}_{H}^{c} \bar{d}_{H}^{c} - \bar{e}_{H}^{c} \bar{u}_{H}^{c} \right) g^{c} + 2\lambda_{\bar{H}} \bar{u}_{H}^{c} \bar{d}_{H}^{c} \bar{g}^{c}, \tag{12}$$

where the color indices have been suppressed and ε is the 2 × 2 antisymmetric matrix with $\varepsilon_{12} = 1$. Let us note, in passing, that the combination of two [three] color-charged objects in a term involves a contraction of the color indices with the symmetric [antisymmetric] invariant tensor δ_{ab} [ε_{abc}], e.g. $u_H^c \bar{u}_H^c = \delta_{ab} u_{Ha}^c \bar{u}_{Hb}^c$ [$u_H^c d_H^c g^c = \varepsilon_{abc} u_{Ha}^c d_{Hb}^c g_c^c$]. Given that H^c and \bar{H}^c in Eq. (9a) acquire their VEVs along the direction of ν_H^c and $\bar{\nu}_H^c$ respectively, it is obvious from Eq. (12) that g^c and \bar{g}^c pair with d_H^c and d_H^c respectively and acquire superheavy masses of order $M_{\rm GUT}$.

The second part $W_{\rm RHN}$ of $W_{\rm M}$ in Eq. (11) provides intermediate scale Majorana masses for ν_i^c as follows:

$$W_{\rm RHN} = \lambda_{ij\nu^c} \bar{H}^c F_i^c \bar{H}^c F_j^c / M_{\rm S}$$

= $\lambda_{ij\nu^c} (\bar{e}_H^c e_i^c + \bar{d}_H^c d_i^c - \bar{\nu}_H^c \nu_i^c - \bar{u}_H^c u_i^c) (\bar{e}_H^c e_i^c + \bar{d}_H^c d_i^c - \bar{\nu}_H^c \nu_i^c - \bar{u}_H^c u_i^c) / M_{\rm S},$ (13)

where $M_{\rm S} \simeq 5 \cdot 10^{17}~{\rm GeV}$ is the string scale. Therefore, the ν_i^c 's acquire Majorana masses of order $M_{\rm GUT}^2/M_{\rm S} \sim 10^{10}-10^{14}~{\rm GeV}$ depending on the magnitude of the coupling constants $\lambda_{ij\nu^c}$.

The last part of $W_{\rm M}$ in Eq. (11), which is responsible for the mixing of the $SU(2)_L$ doublets in Ih and Ih', is a sum of $G_{\rm PS}$ invariants with the traces taken w.r.t. the $SU(4)_{\rm C}$ and $SU(2)_L$ indices:

$$W_{\text{mix}} = M_{h} \text{Tr} \left(\bar{h}' \varepsilon \mathcal{h}'^{\mathsf{T}} \varepsilon \right) + \lambda_{3} \text{Tr} \left(\bar{h}' \varepsilon \phi \mathcal{h}^{\mathsf{T}} \varepsilon \right) + \lambda_{1} \text{Tr} \left(\bar{h}' \varepsilon \phi' \mathcal{h}^{\mathsf{T}} \varepsilon \right). \tag{14}$$

Here the mass parameter M_h is of order $M_{\rm GUT}$ (made real and positive by field rephasing) and λ_3 , λ_1 are dimensionless complex coupling constants. Note that the two last terms in the *right hand side* (RHS) of Eq. (14) overshadow the corresponding ones from the non-renormalizable $SU(2)_R$ -triplet and singlet couplings originating from the symbolic coupling $\bar{H}^cH^c\bar{h}'Ih$ (see Ref. 35).

Replacing ϕ and ϕ' by their VEVs in Eq. (9b) and expanding the superfields in Eq. (5) as linear combinations of the fifteen generators T^a of $SU(4)_c$ normalized so as $\text{Tr}(T^aT^b) = \delta^{ab}$ and denoting the colorless components of the superfields by the superfield symbol, we can easily establish the following identities:

$$\operatorname{Tr}\left(\bar{h}'\varepsilon h'^{\mathsf{T}}\varepsilon\right) = \bar{h}_{1}'^{\mathsf{T}}\varepsilon h_{2}' + h_{1}'^{\mathsf{T}}\varepsilon \bar{h}_{2}' + \cdots, \tag{15a}$$

$$\operatorname{Tr}\left(\bar{lh}'\varepsilon\phi lh^{\mathsf{T}}\right) = \frac{v_{\phi}}{\sqrt{2}}\operatorname{Tr}\left(\bar{lh}'\varepsilon\sigma_{3}lh^{\mathsf{T}}\varepsilon\right) = \left(\bar{lh}_{1}'^{\mathsf{T}}\varepsilon lh_{2} - lh_{1}^{\mathsf{T}}\varepsilon \bar{lh}_{2}'\right),\tag{15b}$$

$$\operatorname{Tr}\left(\bar{l}h'\varepsilon\phi'lh^{\mathsf{T}}\right) = \frac{v'_{\phi}}{\sqrt{2}}\operatorname{Tr}\left(\bar{l}h'\varepsilon\sigma_{0}lh^{\mathsf{T}}\varepsilon\right) = \left(\bar{l}h'_{1}^{\mathsf{T}}\varepsilon lh_{2} + lh'_{1}^{\mathsf{T}}\varepsilon \bar{l}h'_{2}\right),\tag{15c}$$

where the ellipsis includes color nonsinglet components of the superfields. Upon substitution of the above formulas in the RHS of Eq. (14), we obtain the mass terms

$$W_{\text{mix}} = M_{\mathbf{h}} \bar{\mathbf{h}}_{1}^{\prime \mathsf{T}} \boldsymbol{\varepsilon} \left(\mathbf{h}_{2}^{\prime} + \alpha_{2} \mathbf{h}_{2} \right) + M_{\mathbf{h}} \left(\mathbf{h}_{1}^{\prime \mathsf{T}} + \alpha_{1} \mathbf{h}_{1}^{\mathsf{T}} \right) \boldsymbol{\varepsilon} \bar{\mathbf{h}}_{2}^{\prime} + \cdots, \tag{16}$$

where the complex dimensionless parameters α_1 and α_2 are given by

$$\alpha_1 = \frac{1}{\sqrt{2}M_h} \left(-\lambda_3 v_\phi + \lambda_1 v_\phi' \right),\tag{17a}$$

$$\alpha_2 = \frac{1}{\sqrt{2}M_h} \left(\lambda_3 v_\phi + \lambda_1 v_\phi' \right) . \tag{17b}$$

It is obvious from Eq. (16) that we obtain the following two pairs of superheavy doublets with mass M_h

$$\bar{I}h'_1, H'_2 \text{ and } H'_1, \bar{I}h'_2, \text{ where } H'_r = \frac{I\!\!h'_r + \alpha_r I\!\!h_r}{\sqrt{1 + |\alpha_r|^2}}, r = 1, 2.$$
 (18)

The electroweak doublets H_r , which remain massless at the GUT scale, are orthogonal to the H'_r directions:

$$H_r = \frac{-\alpha_r^* \hbar_r' + \hbar_r}{\sqrt{1 + |\alpha_r|^2}}.$$
 (19)

2.4. Yukawa Quasi-Unification Conditions

The part of W in Eq. (6) which includes the Yukawa interactions of the third family of fermions is given by

$$W_{\rm Y} = y_{33} F_3 I h F_3^c + 2y_{33}' F_3 I h' F_3^c = y_{33} F_3 \left(I h_2 + 2\rho I h_2' I h_1 + 2\rho I h_1' \right) F_3^c, \quad (20)$$

where $\rho \equiv y'_{33}/y_{33}$ can be made real and positive by readjusting the phases of Ih, Ih', and H_r . Also, note that the factor of two is incorporated in the second term in the RHS of this equation in order to make y'_{33} directly comparable to y_{33} , since I'_{11} and I'_{12} are proportional to T_c^{15} , which is normalized so that the trace of its square equals unity. Solving Eqs. (18) and (19) w.r.t. Ih_r and Ih'_r , we obtain

$$I h_r = \frac{H_r + \alpha_r^* H_r'}{\sqrt{1 + |\alpha_r|^2}} \text{ and } I h_r' = \frac{-\alpha_r H_r + H_r'}{\sqrt{1 + |\alpha_r|^2}}.$$
(21)

From Eqs. (20) and (21) and using the fact that the superheavy doublets H'_r must have zero VEVs, we can readily derive the superpotential terms of the MSSM for the third family fermions as well as the Yukawa interaction of the left handed third family lepton doublet with ν_3^c :

$$W_{Y} = -h_{t}H_{2}^{\mathsf{T}} \varepsilon Q_{3}u_{3}^{c} + h_{b}H_{1}^{\mathsf{T}} \varepsilon Q_{3}d_{3}^{c} + h_{\tau}H_{1}^{\mathsf{T}} \varepsilon L_{3}e_{3}^{c} - h_{\nu_{\tau}}H_{2}^{\mathsf{T}} \varepsilon L_{3}\nu_{3}^{c}, \tag{22}$$

where $Q_i = \left(u_i \ d_i\right)^\mathsf{T}$ and $L_i = \left(\nu_i \ e_i\right)^\mathsf{T}$ are the $SU(2)_L$ doublet LH quark and lepton superfields respectively and the Yukawa coupling constants h_t, h_b, h_τ , and h_{ν_τ} satisfy a set of generalized asymptotic YQUCs:

$$h_{t}(M_{\text{GUT}}): h_{b}(M_{\text{GUT}}): h_{\tau}(M_{\text{GUT}}): h_{\nu_{\tau}}(M_{\text{GUT}}) = \left| \frac{1 - \rho \alpha_{2} / \sqrt{3}}{\sqrt{1 + |\alpha_{2}|^{2}}} \right| : \left| \frac{1 - \rho \alpha_{1} / \sqrt{3}}{\sqrt{1 + |\alpha_{1}|^{2}}} \right| : \left| \frac{1 + \sqrt{3} \rho \alpha_{1}}{\sqrt{1 + |\alpha_{1}|^{2}}} \right| : \left| \frac{1 + \sqrt{3} \rho \alpha_{2}}{\sqrt{1 + |\alpha_{2}|^{2}}} \right|.$$
 (23)

These conditions depend on two complex (α_1, α_2) and one real and positive (ρ) parameter. For natural values of ρ , α_1 , and α_2 , i.e. for values of these parameters which are of order unity and do not lead to unnaturally small numerators in the RHS of Eq. (23), we expect all the ratios h_m/h_n with $m, n = t, b, \tau, \nu_\tau$ to be of order unity. So, exact YU is naturally broken, but not completely lost since the ratios of the Yukawa coupling constants remain of order unity, thereby restricting $\tan \beta$ to rather large values. On the other hand, these ratios do not have to obey any exact relation among themselves as in the previously studied35-39,41,42 monoparametric case. As we show below, this gives us an extra freedom which allows us to satisfy all the phenomenological and cosmological requirements with the lightest neutralino contributing to CDM.

2.5. The Peccei-Quinn Symmetry and the μ Problem

The last term W_{PO} of W in Eq. (6) is responsible for the solution of the μ problem of MSSM. Indeed, an important shortcoming of MSSM is that there is no understanding of how the SUSY μ term with the right magnitude of $|\mu| \sim 10^2 - 10^3$ GeV arises. One way⁷⁷

to solve this μ problem is via a PQ symmetry $U(1)_{\rm PQ}$, $^{71-73}$ which also solves the strong CP problem. This solution is based on the observation 78 that the axion decay constant f_a , which is the symmetry breaking scale of $U(1)_{\rm PQ}$, is (normally) of intermediate value ($\sim 10^{11}-10^{12}~{\rm GeV}$) and, thus, $|\mu|\sim f_a^2/M_{\rm S}$. The scale f_a is, in turn, of order $(m_{3/2}M_{\rm S})^{1/2}$, where $m_{3/2}\sim 1~{\rm TeV}$ is the gravity-mediated soft SUSY breaking scale (gravitino mass). In order to implement this solution of the μ problem in our model, we introduce 77 a pair of gauge singlet superfields N and \bar{N} (see Table 1) with the following nonrenormalizable couplings in the superpotential – for an alternative class of superpotentials, see 79–83:

$$W_{\rm PQ} = \lambda_{\mu} \frac{N^2 \, l h^2}{M_{\rm S}} + \lambda'_{\mu} \frac{N^2 \, l h'^2}{M_{\rm S}} + \lambda_{\rm PQ} \frac{N^2 \, \bar{N}^2}{M_{\rm S}}.$$
 (24)

Here, λ_{PQ} is taken real and positive by redefining the phases of the superfields N and \bar{N} . After SUSY breaking, the $N^2\bar{N}^2$ term leads to the scalar potential

$$V_{PQ} = \left(m_{3/2}^2 + 4\lambda_{PQ}^2 \left| \frac{N\bar{N}}{M_S} \right|^2 \right) \left[(|N| - |\bar{N}|)^2 + 2|N||\bar{N}| \right]$$

$$+2|A|m_{3/2}\lambda_{PQ} \frac{|N\bar{N}|^2}{M_S} \cos(\epsilon + 2\theta + 2\bar{\theta}),$$
(25)

where A is the dimensionless coefficient of the soft SUSY breaking term corresponding to the superpotential term $N^2\bar{N}^2$ and ϵ , θ , $\bar{\theta}$ are the phases of A, N, \bar{N} respectively. Minimization of $V_{\rm PQ}$ then requires $|N|=|\bar{N}|$, $\epsilon+2\theta+2\bar{\theta}=\pi$ and $V_{\rm PQ}$ takes the form

$$V_{\rm PQ} = 2|N|^2 m_{3/2}^2 \left(4\lambda_{\rm PQ}^2 \frac{|N|^4}{m_{3/2}^2 M_{\rm S}^2} - |A|\lambda_{\rm PQ} \frac{|N|^2}{m_{3/2} M_{\rm S}} + 1 \right).$$
 (26)

For |A| > 4, the absolute minimum of the potential is at

$$|\langle N \rangle| = |\langle \bar{N} \rangle| \equiv \frac{f_a}{2} = \sqrt{m_{3/2} M_{\rm S}} \sqrt{\frac{|A| + \sqrt{|A|^2 - 12}}{12\lambda_{\rm PO}}} \sim \sqrt{m_{3/2} M_{\rm S}}.$$
 (27)

The μ term is generated predominantly via the terms $N^2 \mathbb{h}^2$ and $N^2 \mathbb{h}'^2$ in Eq. (24) with $|\mu| \sim |\langle N \rangle|^2/M_S$, which is of the right magnitude.

The potential $V_{\rm PQ}$ also has a local minimum at $N=\bar{N}=0$, which is separated from the global PQ minimum by a sizable potential barrier, preventing a successful transition from the trivial to the PQ vacuum. This situation persists at all cosmic temperatures after reheating, as has been shown⁴⁸ by considering the one-loop temperature corrections^{84,85} to the scalar potential. We are, thus, obliged to assume that, after the termination of inflation, the system emerges with the appropriate combination of initial conditions so that it is led⁸⁶ to the PQ vacuum.

2.6. Proton Stability

One can assign baryon number B=1/3 [-1/3] to all the color triplets [antitriplets] of the model, which exist not only in F, F^c , but also in H^c, \bar{H}^c, G , and the extra Higgs superfields. Lepton number (L) can then be defined via B-L. Before including the extra Higgs

superfields in Table 1, baryon and lepton number violation originates from the terms:⁴⁸

$$F^c F^c H^c H^c$$
, $F F \bar{H}^c \bar{H}^c Ih Ih$, $F F \bar{H}^c \bar{H}^c \bar{N}^2$ (28)

(as well as the terms containing the combinations $(H^c)^4$, $(\bar{H}^c)^4$), which give couplings like $u^c d^c d^c_H \nu^c_H$ (or $u^c d^c u^c_H e^c_H$), $u d\bar{d}^c_H \bar{\nu}^c_H$ (or $u d\bar{u}^c_H \bar{e}^c_H$) with appropriate coefficients. Also, the terms GH^cH^c and $G\bar{H}^c\bar{H}^c$ give rise to the B (and L) violating couplings $g^cu^c_Hd^c_H$, $\bar{g}^c \bar{u}_H^c \bar{d}_H^c$. All other combinations are B (and L) conserving since all their $SU(4)_c$ 4's are contracted with $\bar{4}$'s.

The dominant contribution to proton decay comes from effective dimension five operators generated by one-loop diagrams with two of the u_H^c , d_H^c or one of the u_H^c , d_H^c and one of the $u^c_H,\,e^c_H$ circulating in the loop. The amplitudes corresponding to these operators are estimated to be at most of order $m_{3/2}M_{\rm GUT}/M_{\rm S}^3 \lesssim 10^{-34}\,{\rm GeV}^{-1}$. This makes the proton practically stable.

After the inclusion of the superfields \mathbb{I}' and $\bar{\mathbb{I}}'$, the couplings

$$FF\bar{H}^c\bar{H}^chh', FF\bar{H}^c\bar{H}^ch'h'$$
 (29)

(as well as the new couplings containing arbitrary powers of the combinations $(H^c)^4$, $(\bar{H}^c)^4$) give rise³⁵ to additional B and L number violation. However, their contribution to proton decay is subdominant to the one arising from the terms of Eq. (28). One can further show³⁵ that the inclusion of the superfields ϕ , $\bar{\phi}$, ϕ' , and $\bar{\phi}'$ also gives a subdominant contribution to the proton decay.

3. The Resulting CMSSM

Below $M_{\rm GUT}$, the particle content of our models reduces to this of MSSM – modulo SM singlets. The Yukawa coupling constants of the models satisfy Eq. (23). To avoid complications with the seesaw mechanism, we neglect in our analysis the effects from $h_{\nu_{\tau}}$ on the renormalization group (RG) running and the SUSY spectrum, although its impact can be sizable.⁸⁷ We specify below the adopted SUSY breaking scheme (Sec. 3.1), describe the derivation of the (s)particle spectrum paying special attention to the two lightest sparticle mass eigenstates (Sec. 3.2), and discuss the fermion masses (Sec. 3.2).

3.1. Soft SUSY Breaking in the CMSSM

The relevant gravity-mediated soft SUSY-breaking terms in the scalar potential are

$$V_{\text{soft}} = m_F^2 |F|^2 - A_t h_t H_2^{\mathsf{T}} \tilde{\epsilon} \tilde{Q}_3 \tilde{u}_3^c + A_b h_b H_1^{\mathsf{T}} \tilde{\epsilon} \tilde{Q}_3 \tilde{d}_3^c + A_\tau h_\tau H_1^{\mathsf{T}} \tilde{\epsilon} \tilde{L}_3 \tilde{e}_3^c - B \mu H_1^{\mathsf{T}} \tilde{\epsilon} H_2 + \text{h.c.} \quad \text{with} \quad F = H_1, \ H_2, \ \tilde{L}_i, \ \tilde{e}_i^c, \ \tilde{Q}_i, \ \tilde{u}_i^c, \ \tilde{d}_i^c,$$
 (30)

where tilde denotes the superpartner and the A-terms for the two light families, although included, are not shown explicitly. The soft gaugino mass terms in the Lagrangian are

$$\mathcal{L}_{\text{gaug}} = \frac{1}{2} \left(M_1 \tilde{B} \tilde{B} + M_2 \sum_{r=1}^{3} \tilde{W}_r \tilde{W}_r + M_3 \sum_{a=1}^{8} \tilde{g}_a \tilde{g}_a + \text{h.c.} \right),$$
(31)

where \tilde{B} , \tilde{W}_r , and \tilde{g}_a are the bino, winos, and gluinos respectively.

The SUSY-breaking parameters A_t, A_b, A_τ, B , and M_α ($\alpha=1,2,3$) are all of the order of the soft SUSY-breaking scale $\sim 1~{\rm TeV}$, but are otherwise unrelated in the general case. However, if we assume that soft SUSY breaking is mediated by *minimal supergravity* (mSUGRA), i.e. supergravity with minimal Kähler potential and minimal gauge kinetic function, we obtain soft terms which are universal 'asymptotically' (i.e. at $M_{\rm GUT}$). More explicitly, mSUGRA implies

• a common mass $M_{1/2}$ for gauginos:

$$M_1(M_{\text{GUT}}) = M_2(M_{\text{GUT}}) = M_3(M_{\text{GUT}}) = M_{1/2},$$
 (32)

• a common mass m_0 for scalars:

Sleptons:
$$m_{\tilde{L}_i}(M_{\text{GUT}}) = m_{\tilde{e}_i^c}(M_{\text{GUT}}) = m_0,$$
 (33a)

$$\text{Squarks: } m_{\tilde{Q}_i}(M_{\text{GUT}}) = m_{\tilde{u}_i^c}(M_{\text{GUT}}) = m_{\tilde{d}_i^c}(M_{\text{GUT}}) = m_0, \quad \text{(33b)}$$

Higgs:
$$m_{H_1}(M_{\text{GUT}}) = m_{H_2}(M_{\text{GUT}}) = m_0,$$
 (33c)

• a common trilinear coupling constant A_0 :

$$A_t(M_{\text{GUT}}) = A_b(M_{\text{GUT}}) = A_\tau(M_{\text{GUT}}) = A_0,$$
 (34)

where again only the third family trilinear coulpings are shown explicitly.

The MSSM supplemented by universal boundary conditions is generally called constrained MSSM (CMSSM). $^{6-9}$ It is true that the mSUGRA implies two more asymptotic relations: $B_0 = A_0 - m_0$ and $m_0 = m_{3/2}$, where $B_0 = B(M_{\rm GUT})$ and $m_{3/2}$ is the (asymptotic) gravitino mass. These extra conditions are usually not included in the CMSSM. Imposing them, we get the so-called very CMSSM, 88,89 which is a very restrictive version of MSSM and will not be considered further here. Therefore, the free parameters of our model are

$$sign \mu$$
, $tan \beta$, $M_{1/2}$, m_0 , and A_0 , (35)

where sign μ is the sign of μ and $\tan \beta = \langle H_2 \rangle / \langle H_1 \rangle$.

In order to proceed with the investigation of the parameter space of the CMSSM, we integrate the two-loop RG equations for the gauge and Yukawa coupling constants and the one-loop ones for the soft SUSY breaking parameters between the SUSY GUT scale $M_{\rm GUT}$ and a common SUSY threshold

$$M_{\rm SUSY} \simeq (m_{\tilde{t}_1} m_{\tilde{t}_2})^{1/2} \ (\tilde{t}_{1,2} \text{ are the stop mass eigenstates})$$
 (36)

determined in consistency with the SUSY spectrum. At $M_{\rm SUSY}$, we impose radiative EWSB and express the values of the parameters μ (up to its sign) and B (or, equivalently, the mass m_A of the CP-odd neutral Higgs boson A) at $M_{\rm SUSY}$ in terms of the other input parameters by minimizing the tree-level RG improved potential 90,91 at $M_{\rm SUSY}$. The resulting conditions are

$$\mu^2 = \frac{m_{H_1}^2 - m_{H_2}^2 \tan^2 \beta}{\tan^2 \beta - 1} - \frac{1}{2} M_Z^2, \quad \sin 2\beta = \frac{2B\mu}{m_1^2 + m_2^2} \equiv \frac{2B\mu}{m_A^2}, \tag{37}$$

where $m_A^2 = m_1^2 + m_2^2$ with $m_1^2 = m_{H_1}^2 + \mu^2$ and $m_2^2 = m_{H_2}^2 + \mu^2$. We could improve the accuracy of these conditions by including the full one-loop radiative corrections to the potential from Ref. 90,91 at $M_{\rm SUSY}$. It is shown, ^{92,93} however, that the corrections to μ and m_A from the full one-loop effective potential are minimized by our choice of $M_{\rm SUSY}$. So, we will not include these corrections, but rather use this variable SUSY threshold which gives a much better accuracy than a fixed one.

We then evaluate the SUSY spectrum by employing the publicly available calculator SOFTSUSY⁹⁴ and incorporate the SUSY corrections to the b and τ mass.^{90,91} The corrections to the b-quark mass arise from sbottom-gluino (mainly) and stop-chargino $loops^{18,19,90,91}$ and have the sign of μ – with the standard sign convention of Ref. 95. Less important but not negligible (almost 4%) are the SUSY corrections to the τ -lepton mass originating 90,91 from sneutrino-chargino (mainly) and stau-neutralino loops and leading^{35,36} to a small decrease of tan β . From M_{SUSY} to M_Z , the running of the gauge and Yukawa coupling constants is continued using the SM RG equations.

3.2. The LSP and the Next-to-LSP

We now focus on the two lightest sparticles whose mass proximity plays a crucial role in constructing a viable CDM scenario - see Sec. 5. In particular, the role of the LSP can be played by the lightest neutralino $\tilde{\chi}$, whereas the *next-to-LSP* (NLSP) can be the lightest stau mass eigenstate $\tilde{\tau}_2$. Moreover, for presentation purposes, $M_{1/2}$ and m_0 can sometimes be replaced 96,97 by the LSP mass $m_{\rm LSP}$ and the relative mass splitting $\Delta_{\tilde{\tau}_2}$ between $\tilde{\chi}$ and $\tilde{\tau}_2$ defined as follows:

$$\Delta_{\tilde{\tau}_2} = (m_{\tilde{\tau}_2} - m_{\rm LSP})/m_{\rm LSP}.\tag{38}$$

The LSP mass $m_{\rm LSP}$ can be obtained by diagonalizing the mass matrix of the four neutralinos, which is

$$\begin{pmatrix}
M_{1} & 0 & -M_{Z}s_{W}\cos\beta & M_{Z}s_{W}\sin\beta \\
0 & M_{2} & M_{Z}c_{W}\cos\beta & -M_{Z}c_{W}\sin\beta \\
-M_{Z}s_{W}\cos\beta & M_{Z}c_{W}\cos\beta & 0 & -\mu \\
M_{Z}s_{W}\sin\beta & -M_{Z}c_{W}\sin\beta & -\mu & 0
\end{pmatrix} (39)$$

in the $(-i\tilde{B}, -i\tilde{W}_3, \tilde{H}_1, \tilde{H}_2)$ basis. Here, $s_W = \sin\theta_W$, $c_W = \cos\theta_W$, and M_1, M_2 are the masses of \tilde{B} , \tilde{W}_3 in Eq. (31). In the CMSSM and for most of the parameter space, $m_{\rm LSP} \simeq M_1$ and, thus, $\tilde{\chi}$ turns out to be an almost pure bino \tilde{B} .

The evolution of the gaugino masses M_{α} at one loop can be easily found by solving the relevant RG equations, 6-9 which admit an exact solution:

$$M_{\alpha}(Q) = M_{1/2} \frac{g_{\alpha}(Q)}{g_{\text{GUT}}} = M_{1/2} \left(1 - \frac{b_{\alpha}}{8\pi^2} \ln \frac{Q}{M_{\text{GUT}}} \right)^{-1},$$
 (40)

where $(b_{\alpha}) = (33/5, 1, -3)$, g_{α} are the gauge coupling constants associated with the gauge groups $U(1)_Y$, $SU(2)_L$, and $SU(3)_c$ respectively, and $g_{GUT} \simeq 1/24$ is the common value of the g_{α} 's at the GUT scale $M_{\rm GUT} \simeq 2 \times 10^{16}$ GeV. After a direct computation, we obtain $m_{\rm LSP}(M_{\rm SUSY}) \simeq 0.45 M_{1/2}$.

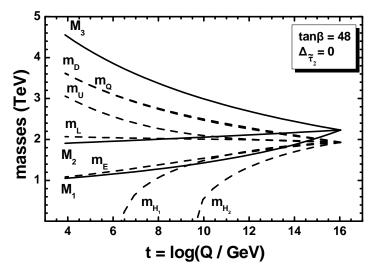


Fig. 1. The RG evolution from $Q=M_{\rm SUSY}$ to $Q=M_{\rm GUT}$ of the soft SUSY-breaking masses of the Higgs bosons $(m_{H_1}$ and m_{H_2}), the third generation scalars $(m_U, m_D, m_E, m_Q,$ and $m_L)$, and the gauginos $(M_1, M_2,$ and $M_3)$ for $\tan\beta=48$, $\Delta_{\tilde{\tau}_2}\simeq 0$, $A_0/M_{1/2}=-1.4$, and $M_{1/2}=2.2~{\rm TeV}$.

The lightest stau mass eigenstate $\tilde{\tau}_2$ can be obtained by diagonalizing the stau mass-squared matrix

$$\begin{pmatrix}
m_{\tau}^{2} + m_{L}^{2} + M_{Z}^{2}(-\frac{1}{2} + s_{W}^{2})\cos 2\beta & m_{\tau}(A_{\tau} - \mu \tan \beta) \\
m_{\tau}(A_{\tau} - \mu \tan \beta) & m_{\tau}^{2} + m_{E}^{2} - M_{Z}^{2}s_{W}^{2}\cos 2\beta
\end{pmatrix}$$
(41)

in the gauge basis $(\tilde{\tau}_L, \ \tilde{\tau}_R)$. Here, $m_{\tilde{\tau}_{L[R]}}$ is the soft SUSY-breaking mass of the left [right] handed stau $\tilde{\tau}_{L[R]}$, m_{τ} the tau-lepton mass, and the simplifying notation $m_L \equiv m_{\tilde{L}_3}$ and $m_E \equiv m_{\tilde{e}_3^c}$ for the third generation soft SUSY-breaking slepton masses is used. The stau mass eigenstates are

$$\begin{pmatrix} \tilde{\tau}_1 \\ \tilde{\tau}_2 \end{pmatrix} = \begin{pmatrix} \cos \theta_{\tilde{\tau}} & \sin \theta_{\tilde{\tau}} \\ -\sin \theta_{\tilde{\tau}} & \cos \theta_{\tilde{\tau}} \end{pmatrix} \begin{pmatrix} \tilde{\tau}_L \\ \tilde{\tau}_R \end{pmatrix},$$
(42)

where $\theta_{\tilde{\tau}}$ is the $\tilde{\tau}_{L} - \tilde{\tau}_{R}$ mixing angle. The large values of the b and τ Yukawa coupling constants, implied by the YQUCs, cause soft SUSY-breaking masses of the third generation squarks and sleptons to run (at low energies) to lower physical values than the corresponding masses of the first and second generation. Furthermore, the large values of $\tan \beta$, implied again by YQUCs, lead to large off-diagonal mixings in the sbottom and stau mass-squared matrices. These effects reduce further the physical $m_{\tilde{\tau}_2}$, which becomes easily the NLSP.

In Fig. 1, an example of the RG running from $Q=M_{\rm SUSY}$ to $Q=M_{\rm GUT}$ of the soft SUSY-breaking masses of the Higgs and the third generation scalars as well as the gauginos is shown. Here, we extend the simplifying notation for the soft masses to include the masses of the third generation squarks too: $m_Q \equiv m_{\tilde{Q}_3}$, $m_U \equiv m_{\tilde{u}_3}$, and $m_D \equiv m_{\tilde{d}_3}$

and take $\tan \beta = 48$, $\Delta_{\tilde{\tau}_2} \simeq 0$, $A_0/M_{1/2} = -1.4$, and $M_{1/2} = 2.2$ TeV resulting to $\mu = 2.78$ TeV. It is rather amazing that, from so few inputs, all of the masses of the SUSY particles can be determined. One characteristic feature of the spectrum which is obvious from this figure is that the colored sparticles are typically the heaviest particles. This is due to the large enhancement of their masses originating from the $SU(3)_c$ gauge coupling g_3 in the RG equations. Also, one sees that $\tilde{\chi}$ can typically play the role of the LSP. Most importantly, though, one notices that $m_{H_1}^2$ and $m_{H_2}^2$ reach zero and then become negative triggering the EWSB. In particular, we obtain $m_1^2(M_{SUSY}) = 4.41 \text{ TeV}^2 > 0$, but $m_2^2(M_{\rm SUSY}) = -2.2 \,{\rm TeV^2} < 0$ and so the quadratic part of the scalar potential for the electrically neutral components of the Higgs fields becomes indefinite – see e.g. Ref. 98 – causing the EWSB.

3.3. The Masses of the Fermions

The masses of the fermions of the third generation play a crucial role in the determination of the evolution of the Yukawa coupling constants. For the b-quark mass, we adopt as an input parameter in our analysis the $\overline{\rm MS}$ b-quark mass, which at $1-\sigma$ is 99

$$m_b (m_b)^{\overline{\rm MS}} = 4.19^{+0.18}_{-0.06} \,\text{GeV}.$$
 (43)

This range is evolved up to M_Z using the central value $\alpha_s(M_Z) = 0.1184^{99}$ of the strong fine structure constant at M_Z and then converted to the $\overline{\rm DR}$ scheme in accordance with the analysis of Ref. 100, 101. We obtain, at 95% c.l.,

$$2.745 \le m_b(M_Z)/\text{GeV} \le 3.13$$
 (44)

with the central value being $m_b(M_Z)=2.84$ GeV. For the top-quark mass, we use the central pole mass (M_t) as an input parameter: $^{102,\,103}$

$$M_t = 173 \text{ GeV} \implies m_t(m_t) = 164.6 \text{ GeV}$$
 (45)

with $m_t(m_t)$ being the running mass of the top quark. We also take the central value $m_{\tau}(M_Z)=1.748~{\rm GeV^{100,\,101}}$ of the $\overline{\rm DR}$ tau-lepton mass at M_Z .

In Fig. 2, we present an example of a third generation Yukawa coupling constant RG running from $M_{\rm GUT}$ to M_Z for $\tan \beta = 48$, $A_0/M_{1/2} = -1.4$, $M_{1/2} = 2.27$ TeV, and $m_0 = 1.92 \text{ TeV}$. At $M_{\rm GUT}$, we have $h_t/h_\tau = 1.117$, $h_b/h_\tau = 0.623$, and $h_t/h_b = 1.792$. This is, actually, the first out of the four cases of Table 2 (see below). As we show in Sec. 7, these ratios can be naturally obtained from the YQUCs in Eq. (23). The kinks on the various curves correspond to the point where the MSSM RG equations are replaced by the SM ones. We observe that h_{τ} is greater than h_b but lower than h_t at M_{GUT} .

4. Phenomenological Constraints

The model parameters are restricted by a number of phenomenological and cosmological constraints, which are evaluated by employing the latest version of the publicly available code micrOMEGAs. 104, 105 We briefly discuss below the phenomenological constraints paying special attention to those which are most relevant to our investigation.

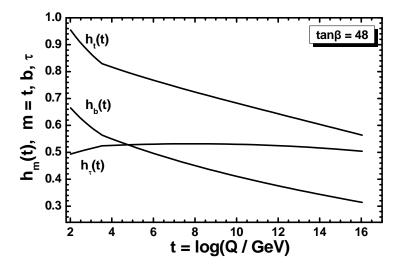


Fig. 2. The RG evolution from $Q=M_Z$ to $Q=M_{\rm GUT}$ of the third generation Yukawa coupling constants for $\tan\beta=48,~A_0/M_{1/2}=-1.4,~M_{1/2}=2.27~{\rm TeV}$, and $m_0=1.92~{\rm TeV}$.

4.1. The Higgs Boson Mass

According to recent independent announcements from the ATLAS⁶² and the CMS⁶³ experimental teams at the LHC – see also Ref. 64 – a discovered particle, whose behavior is consistent with the SM Higgs boson, has a mass around 125-126 GeV. More precisely, the reported mass is

$$m_h = \begin{cases} 126.0 \pm 0.4 \text{ (stat)} \pm 0.4 \text{ (sys) GeV ATLAS,} \\ 125.3 \pm 0.4 \text{ (stat)} \pm 0.5 \text{ (sys) GeV CMS.} \end{cases}$$
(46)

In the absence of a combined analysis of the ATLAS and CMS data and allowing for a theoretical uncertainty of ± 1.5 GeV, we construct a $2-\sigma$ range for m_h adding in quadrature the various experimental and theoretical uncertainties and taking the upper [lower] bound from the ATLAS [CMS] results:

$$122 \lesssim m_h/\text{GeV} \lesssim 129.2.$$
 (47)

This restriction is applied to the mass m_h of the light CP-even Higgs boson h of MSSM. For the calculation of m_h , we use the package SOFTSUSY, ⁹⁴ which includes the full one-loop SUSY corrections and some zero-momentum two-loop corrections. ^{106–109} The results are well tested ^{110,111} against other spectrum calculators.

In Fig. 3, we depict m_h as a function of $m_{\rm LSP}$ for $\tan\beta=48$, $\Delta_{\tilde{\tau}_2}\simeq0$, and $A_0/M_{1/2}=1,\,0,\,-1,$ and -1.5. We notice that m_h increases with $m_{\rm LSP}$ and as $A_0/M_{1/2}$ decreases to values lower than zero. This occurs, since the off-diagonal elements of the mass-squared matrix of the stop quarks, which contribute to the corrections to m_h , are maximized for $A_0/M_{1/2}<0$. As a consequence, the bound on $m_{\rm LSP}$ for $A_0/M_{1/2}<0$ turns out to be less restrictive.

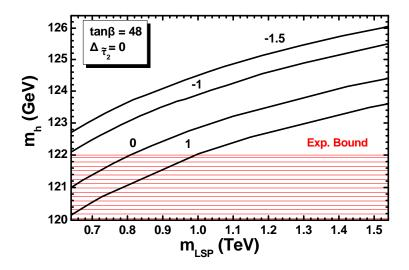


Fig. 3. The mass m_h of the MSSM Higgs boson as a function of $m_{\rm LSP}$ for $\tan\beta=48,\ \Delta_{\tilde{\tau}_2}\simeq 0$, and various $A_0/M_{1/2}$'s indicated in the plot. The (red) region is excluded by the lower bound in Eq. (47).

4.2. The Branching Ratio BR $(B_s \to \mu^+\mu^-)$

The rare decay $B_s \to \mu^+\mu^-$ occurs via Z penguin and box diagrams in the SM and, thus, its branching ratio is highly suppressed. The SUSY contribution, though, originating¹¹²⁻¹¹⁷ from neutral Higgs bosons in chargino-, H^{\pm} -, and W^{\pm} -mediated penguins behaves as $\tan^6 \beta/m_A^4$ and hence is particularly important for large $\tan \beta$'s. We impose here the following 95% c.l. bound^{65,66}

BR
$$(B_s \to \mu^+ \mu^-) \lesssim 4.2 \times 10^{-9}$$
, (48)

which is significantly reduced relative to the previous experimental upper bound. 118 This bound implies a lower bound on $m_{\rm LSP}$, since BR $(B_s \to \mu^+ \mu^-)$ decreases as $m_{\rm LSP}$ increases. Note that, very recently, the LHCb collaboration reported¹¹⁹ a first evidence for the decay $B_s \to \mu^+\mu^-$ yielding the following two sided 95% c.l. bound

$$1.1 \lesssim BR (B_s \to \mu^+ \mu^-)/10^{-9} \lesssim 6.4.$$
 (49)

In spite of this newer experimental upper bound on BR $(B_s \to \mu^+ \mu^-)$, we adopt here the much tighter upper bound on BR $(B_s \to \mu^+\mu^-)$ in Eq. (48), since it is a combined result⁶⁸ of the ATLAS, CMS, and LHCb experiments and, thus, more realistic. As we show below, the upper bound on the LSP mass $m_{\rm LSP}$ which can be inferred from the lower bound on BR $(B_s \to \mu^+ \mu^-)$ in Eq. (49) does not constrain the parameters of our model.

In Fig. 4, we depict BR $(B_s \to \mu^+ \mu^-)$ as a function of $m_{\rm LSP}$ for $\tan \beta = 48, \ \Delta_{\tilde{\tau}_2} \simeq 0$ and $A_0/M_{1/2}=1,\ 0,\ -1,$ and -1.5. We observe that BR $(B_s\to\mu^+\mu^-)$ decreases as $m_{\rm LSP}$ and $A_0/M_{1/2}$ increase. Therefore, for $A_0/M_{1/2} < 0$, which is favored by the data on m_h , the bound on $m_{\rm LSP}$ from Eq. (48) is more restrictive than for $A_0/M_{1/2} > 0$.

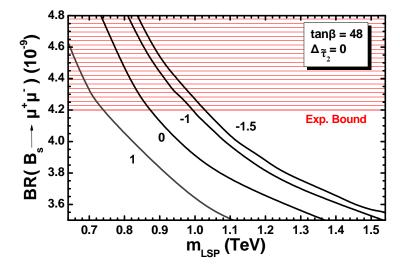


Fig. 4. BR $(B_s \to \mu^+ \mu^-)$ as a function of $m_{\rm LSP}$ for $\tan \beta = 48$, $\Delta_{\tilde{\tau}_2} \simeq 0$, and various $A_0/M_{1/2}$'s indicated in the plot. The experimentally excluded (red) region is also shown.

4.3. The Branching Ratio BR $(b \rightarrow s\gamma)$

Combining in quadrature the experimental and theoretical errors in the most recent experimental world average ¹²⁰ and the SM prediction ¹²¹ for the branching ratio BR $(b \to s\gamma)$ of the process $b \to s\gamma$, we obtain the following constraints at 95% c.l.:

$$2.84 \times 10^{-4} \lesssim BR(b \to s\gamma) \lesssim 4.2 \times 10^{-4}$$
. (50)

The computation of BR $(b \to s \gamma)$ in the micromegas package presented in Ref. 122 includes 123–126 next-to-leading order (NLO) QCD corrections to the charged Higgs boson (H^\pm) contribution, the $\tan\beta$ enhanced contributions, and resummed NLO SUSY QCD corrections. The H^\pm contribution interferes constructively with the SM contribution, whereas the SUSY contribution interferes destructively with the other two contributions for $\mu>0$. The SM contribution plus the H^\pm and SUSY contributions initially increases with $m_{\rm LSP}$ and yields a lower bound on $m_{\rm LSP}$ from the lower bound in Eq. (50). For higher values of $m_{\rm LSP}$, it starts mildly decreasing.

4.4. The Ratio R $(B_u \to \tau \nu)$

The purely leptonic decay $B_u \to \tau \nu$ proceeds via W^\pm - and H^\pm -mediated annihilation processes. The SUSY contribution, contrary to the SM one, is not helicity suppressed and depends on the mass m_{H^\pm} of the charged Higgs boson since it behaves 117,127,128 like $\tan^4\beta/m_{H^\pm}^4$. The ratio $\mathrm{R}\,(B_u\to\tau\nu)$ of the CMSSM to the SM branching ratio of the process $B_u\to\tau\nu$ increases with m_{LSP} and approaches unity. It is to be consistent with the following 95% c.l. range: 120

$$0.52 \lesssim R \left(B_u \to \tau \nu \right) \lesssim 2.04 \,. \tag{51}$$

A lower bound on $m_{\rm LSP}$ can be derived from the lower bound in this inequality.

4.5. Muon Anomalous Magnetic Moment

The discrepancy δa_{μ} between the measured value a_{μ} of the muon anomalous magnetic moment and its predicted value in the SM can be attributed to SUSY contributions arising from chargino-sneutrino and neutralino-smuon loops. The relevant calculation is based on the formulas of Ref. 129. The absolute value of the result decreases as $m_{\rm LSP}$ increases and its sign is positive for $\mu > 0$. On the other hand, the calculation of $a_{\mu}^{\rm SM}$ is not yet stabilized mainly because of the ambiguities in the calculation of the hadronic vacuumpolarization contribution. According to the evaluation of this contribution in Ref. 20, there is still a discrepancy between the findings based on the e^+e^- -annihilation data and the ones based on the τ -decay data – however, in Ref. 23, it is claimed that this discrepancy can be alleviated. Taking into account the more reliable calculation based on the e^+e^- data, ²¹ the recent complete tenth-order QED contribution, 22 and the experimental measurements 130 of a_{μ} , we end up with a $2.9 - \sigma$ discrepancy

$$\delta a_{\mu} = (24.9 \pm 8.7) \times 10^{-10},$$
 (52)

resulting to the following 95% c.l. range:

$$7.5 \times 10^{-10} \lesssim \delta a_{\mu} \lesssim 42.3 \times 10^{-10}$$
. (53)

A lower [upper] bound on $m_{\rm LSP}$ can be derived from the upper [lower] bound in Eq. (53). As it turns out, only the upper bound on m_{LSP} is relevant here. Taking into account the aforementioned computational instabilities and the fact that a discrepancy at the level of about $3-\sigma$ cannot firmly establish a real deviation from the SM value, we do not consider this bound as a strict constraint, but rather restrict ourselves to just mentioning at which level Eq. (52) is satisfied in the parameter space of the model allowed by all the other constraints - cf. Ref. 131-133.

5. Cold Dark Matter Considerations

The Lagrangian of MSSM is invariant under a discrete $\mathbb{Z}_2^{\mathrm{mp}}$ 'matter parity' symmetry, under which all 'matter' (i.e. quark and lepton) superfields change sign – see Table 1. Combining this symmetry with the \mathbb{Z}_2 fermion number symmetry, under which all fermions change sign, we obtain the discrete \mathbb{Z}_2 R-parity symmetry, under which all SM particles are even, while all sparticles are odd. By virtue of R-parity conservation, the LSP is stable and, thus, can contribute to the CDM in the universe. It is important to note that matter parity is vital for MSSM to avoid baryon- and lepton-number-violating renormalizable couplings in the superpotential, which would lead to highly undesirable phenomena such as very fast proton decay. So, the possibility of having the LSP as CDM candidate is not put in by hand, but arises naturally from the very structure of MSSM.

The 95% c.l. range for the CDM abundance, according to the results of WMAP, 67 is

$$\Omega_{\rm CDM}h^2 = 0.1126 \pm 0.0072. \tag{54}$$

The LSP ($\tilde{\chi}$) can be a viable CDM candidate if its relic abundance $\Omega_{\rm LSP}h^2$ does not exceed the 95% c.l. upper bound derived from Eq. (54), i.e.

$$\Omega_{\rm LSP} h^2 \lesssim 0.12.$$
(55)

Note that, in accordance with the recently reported 134 results from the Planck satellite, the CDM abundance is slightly larger. This leads to an upper bound on $\Omega_{\rm LSP}h^2$ which is somewhat less restrictive than the one we use in our calculation. The lower bound on $\Omega_{\rm LSP}h^2$ is not taken into account in our analysis, since other production mechanisms $^{135-138}$ of LSPs may be present too and/or other particles $^{139-143}$ may also contribute to the CDM. We calculate $\Omega_{\rm LSP}h^2$ using the micromegas code, which includes accurately thermally averaged exact tree-level cross sections of all the (co)annihilation processes, 96,97,144,145 treats poles $^{35,146-149}$ properly, and uses one-loop QCD and SUSY QCD corrected 18,19,35,122 Higgs decay widths and couplings to fermions.

The bound in Eq. (55) strongly restricts the parameters of the CMSSM, since $\Omega_{\rm LSP}h^2$ generally increases with the mass $m_{\rm LSP}$ of the LSP and so an upper bound on $m_{\rm LSP}$ can be derived from this equation. Actually, in most of the parameter space of the CMSSM, $\Omega_{\rm LSP}h^2$ turns out to be greater than the bound in Eq. (55) and can become compatible with this equation mainly in the following clearly distinguished regions (or 'islands') in the CMSSM parameter space:

- in the bulk region which appears at low values of m_0 and $M_{1/2}$, where $\tilde{\chi}\tilde{\chi}$ annihilation occurs predominantly via t-channel slepton exchange. This region is now excluded by the bound in Eq. (47).
- in the hyperbolic branch/focus point (HB/FP) region, which lies at large values of m_0 (> 5 TeV), where $|\mu|$ becomes small and the neutralino $\tilde{\chi}$ develops a significant higgsino component 150–156 (for some details, see Sec. 8).
- in the stau coannihilation tail at low m_0 's but almost any value of $M_{1/2}$, where there is a proximity between the masses of the LSP and the NLSP, which turns out to be the $\tilde{\tau}_2$ for $\tan\beta>10^{144,145}$ and not too large values of $|A_0|$. Large $|A_0|$ can generate a stop coannihilation region. For fixed $m_{\rm LSP}$, $\Omega_{\rm LSP}h^2$ decreases with $\Delta_{\tilde{\tau}_2}$, since the $\tilde{\chi}\tilde{\tau}_2$ coannihilations become more efficient. So the CDM criterion can be used for restricting $\Delta_{\tilde{\tau}_2}$ see Refs. 35, 37, 38, 96, 97.
- in the A-pole enhanced $\tilde{\chi}\tilde{\chi}$ annihilation funnel for $\tan\beta > 40 \ [\tan\beta \simeq 30 35]$ for $\mu > 0 \ [\mu < 0]$, where one encounters the presence of a resonance with

$$\Delta_A \equiv \left(m_A - 2m_{\rm LSP} \right) / 2m_{\rm LSP} \simeq 0 \tag{56}$$

in the $\tilde{\chi}\tilde{\chi}$ annihilation to down type fermions via a s-channel exchange of an A-boson.

In the region of the CMSSM parameter space which is favored by the bound in Eq. (47) with $A_0/M_{1/2} < 0$, it is recently recognized^{69,131–133} that there is an area where two $\Omega_{\rm LSP}h^2$ reduction mechanisms analogous to the two latter ones mentioned just above cooperate to reduce the LSP relic abundance below 0.12. In particular, the lines $\Delta_{\tilde{\tau}_2} = 0$ and $\Delta_A = 0$ can intersect each other in this area, leading to a resonant enhancement of the

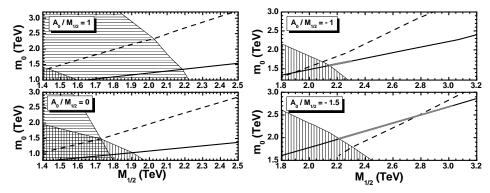


Fig. 5. Relative position of the $\Delta_{\tilde{\tau}_2}=0$ (solid) line and the $\Delta_H=0$ (dashed) line in the $M_{1/2}-m_0$ plane for tan $\beta = 48$ and various values of $A_0/M_{1/2}$ indicated in the graphs. The vertically [horizontally] hatched regions are excluded by the bound in Eq. (48) [lower bound in Eq. (47)]. The gray areas are the overall allowed areas

 $\tilde{\chi}\tilde{\tau}_2$ coannihilations. Note that, since $m_A \simeq m_H$, where m_H is the mass of the heavy CPeven neutral Higgs boson H, $\Delta_A \simeq 0$ implies the presence of a resonance $2m_{\rm LSP} \simeq m_H$ too. Under these circumstances, the $\tilde{\tau}_2\tilde{\tau}_2^*$ coannihilations to bb and $\tau\bar{\tau}$ are enhanced by the s-channel exchange of a H-pole – for the relevant channels, see, for example, Ref. 96, 97.

In order to pinpoint more precisely this effect, we track in Fig. 5 the relative position of the lines $\Delta_{\tilde{\tau}_2} = 0$ and $\Delta_H \equiv (m_H - 2m_{\rm LSP})/2m_{\rm LSP} = 0$ in the $M_{1/2} - m_0$ plane for $\tan \beta = 48$ and various values of $A_0/M_{1/2}$. The solid [dashed] lines correspond to $\Delta_{\tilde{\tau}_2} = 0$ [$\Delta_H = 0$]. Also, the vertically [horizontally] hatched regions are excluded by the bound on BR $(B_s \to \mu^+ \mu^-)$ in Eq. (48) [lower bound on m_h in Eq. (47)]. We observe that, for $A_0/M_{1/2}=1$, the lower bound on $M_{1/2}$ which originates from the lower bound on m_h in Eq. (47) overshadows the one from Eq. (48). In all other cases, however, we have the opposite situation. This is consistent with the fact that, for almost fixed $M_{1/2}$ and m_0 , m_h increases as $A_0/M_{1/2}$ decreases – see Fig. 3.

From Fig. 5, we see that, for $A_0/M_{1/2}=1$ and 0, the $\Delta_H=0$ line is far from the part of the $\Delta_{\tilde{\tau}_2} = 0$ line which is allowed by all the other constraints except the CDM bound. Consequently, in the neighborhood of this part, the effect of the H-pole is not strong enough to reduce $\Omega_{\rm LSP}h^2$ below 0.12 via $\tilde{\tau}_2\tilde{\tau}_2^*$ coannihilations and no overall allowed area exists. On the contrary, for $A_0/M_{1/2}=-1$, the $\Delta_H=0$ line gets near the otherwise allowed (i.e. allowed by all the other requirements in Sec. 4 without considering the CDM bound) part of the $\Delta_{\tilde{\tau}_2} = 0$ line and starts affecting the neighborhood of its leftmost segment, where $\Omega_{\rm LSP}h^2$ becomes smaller than 0.12 and, thus, an overall allowed (gray) area appears. For $A_0/M_{1/2}=-1.5$, the $\Delta_H=0$ line moves downwards and intersects the $\Delta_{\tilde{\tau}_2}=0$ line. This enhances H-pole $\tilde{\tau}_2\tilde{\tau}_2^*$ coannihilation in the neighborhood of a bigger segment of the otherwise allowed part of the $\Delta_{\tilde{\tau}_2} = 0$ line, where $\Omega_{\rm LSP} h^2$ is reduced below 0.12, and, thus, a bigger overall allowed (gray) area is generated. For even smaller $A_0/M_{1/2}$'s, the $\Delta_H = 0$ line keeps moving downwards and gets away from most of the otherwise allowed part of the $\Delta_{\tilde{\tau}_2} = 0$ line. Also, the intersection of these two lines moves to higher values of

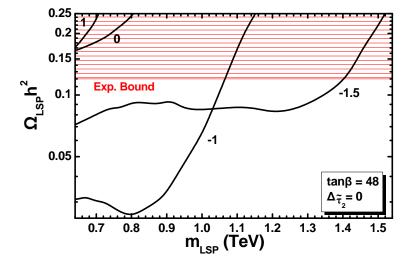


Fig. 6. $\Omega_{\rm LSP}h^2$ as a function of $m_{\rm LSP}$ for $\tan\beta=48$, $\Delta_{\tilde{\tau}_2}\simeq 0$, and various $A_0/M_{1/2}$'s indicated in the graph. The experimentally excluded (red) area is also depicted.

 $M_{1/2}$ and m_0 and the effect of the H-pole is weakened even around this intersection. As a consequence, the overall allowed area quickly disappears as $A_0/M_{1/2}$ moves below -1.6, as we will see in Sec. 6.

The effect of the H-pole on $\Omega_{\rm LSP}h^2$ can be further highlighted by considering Fig. 6, where we depict $\Omega_{\rm LSP}h^2$ as a function of $m_{\rm LSP}$ for $\tan\beta=48$, $\Delta_{\tilde{\tau}_2}\simeq 0$, and $A_0/M_{1/2}=1$, 0,-1, and -1.5. We notice that, for $A_0/M_{1/2}\geq 0$, $\Omega_{\rm LSP}h^2$ is always greater than 0.12 and increases sharply with $m_{\rm LSP}$. On the contrary, for $A_0/M_{1/2}<0$, $\Omega_{\rm LSP}h^2$ can be smaller than 0.12 with an almost flat plateau. More precisely, we see that $\Omega_{\rm LSP}h^2$ remains almost constant and lower than 0.12 when $m_{\rm LSP}$ is lower than its value $m_{\rm LSP}^c$ at which the $\Delta_H=0$ line intersects the $\Delta_{\tilde{\tau}_2}=0$ line – recall that $m_{\rm LSP}\simeq 0.45M_{1/2}$. From our code, we estimate that $m_{\rm LSP}^c\simeq 0.8$ TeV [$m_{\rm LSP}^c\simeq 1.25$ TeV] for $A_0/M_{1/2}=-1$ [$A_0/M_{1/2}=-1.5$]. At $m_{\rm LSP}=m_{\rm LSP}^c$, we get a mild temporary reduction of $\Omega_{\rm LSP}h^2$, whereas, for $m_{\rm LSP}>m_{\rm LSP}^c$, $\Omega_{\rm LSP}h^2$ increases sharply.

6. Restrictions on the Supersymmetry Parameters

Imposing the requirements described in Secs. 4 and 5, we can delineate the allowed parameter space of our model. We find that the only constraints which play a role are the CDM bound in Eq. (55), the lower bound on m_h in Eq. (47), and the bound on BR $(B_s \to \mu^+ \mu^-)$ in Eq. (48). In the parameter space allowed by these requirements, all the other restrictions of Sec. 4 are automatically satisfied with the exception of the lower bound on δa_μ in Eq. (53). This bound is not imposed here as a strict constraint on the parameters of the model for the reasons explained in Sec. 4.5. We only discuss at which level Eq. (52) is satisfied in the parameter space allowed by all the other requirements.

Initially, we concentrate on a representative value of $\tan \beta = 48$ and delineate the

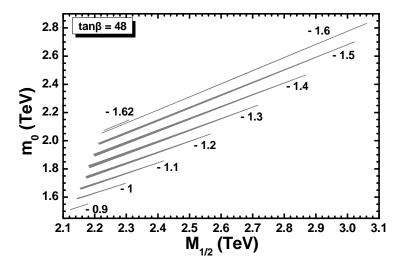


Fig. 7. The allowed (shaded) areas in the $M_{1/2} - m_0$ plane for $\tan \beta = 48$ and various $A_0/M_{1/2}$'s indicated in the graph.

allowed areas in the $M_{1/2} - m_0$ plane for various values of $A_0/M_{1/2}$. These allowed areas are the shaded ones in Fig. 7. We observe that these areas are very thin strips. Their lower boundary corresponds to $\Delta_{\tilde{\tau}_2} = 0$. The area below this boundary is excluded because the LSP is the charged $\tilde{\tau}_2$. The upper boundary of the areas comes from the CDM bound in Eq. (55), while the left one originates from the limit on BR $(B_s \to \mu^+ \mu^-)$ in Eq. (48). The upper right corner of the areas coincides with the intersection of the lines $\Delta_{\tilde{\tau}_2} = 0$ and $\Omega_{\rm LSP}h^2=0.12$. We observe that the allowed area, starting from being just a point at a value of $A_0/M_{1/2}$ slightly bigger than -0.9, gradually expands as $A_0/M_{1/2}$ decreases and reaches its maximal size around $A_0/M_{1/2}=-1.6$. For smaller $A_0/M_{1/2}$'s, it shrinks very quickly and disappears just after $A_0/M_{1/2}=-1.62$. We find that, for $\tan\beta=48$, $m_{\rm LSP}$ ranges from about 983 to 1433 GeV, while m_h ranges from about 123.7 to 125.93 GeV.

To get a better idea of the allowed parameter space, we focus on the coannihilation regime and construct the allowed region in the $M_{1/2} - A_0/M_{1/2}$ plane. This is shown in Fig. 8, where we depict the (horizontally hatched) areas allowed by the various constraints for $\Delta_{\tilde{\tau}_2}=0$ and various values of $\tan\beta$ indicated in the graph. This choice ensures the maximal possible reduction of $\Omega_{LSP}h^2$ due to the $\tilde{\chi}\tilde{\tau}_2$ coannihilation. So, for $\Delta_{\tilde{\tau}_2}=0$, we find the maximal $M_{1/2}$ or $m_{\rm LSP}$ allowed by Eq. (55) for a given value of $A_0/M_{1/2}$. The right boundaries of the allowed regions correspond to $\Omega_{LSP}h^2=0.12$, while the left ones saturate the bound on BR $(B_s \to \mu^+ \mu^-)$ in Eq. (48) – cf. Fig. 9. The almost horizontal upper boundaries correspond to the sudden shrinking of the allowed areas which, as already discussed, is due to the weakening of the H-pole effect as $A_0/M_{1/2}$ drops below a certain value for each $\tan \beta$. The lower left boundary of the areas for $\tan \beta = 44, 45,$ and 46 comes for the lower bound on m_h in Eq. (47), while the somewhat curved, almost horizontal, part of the lower boundary of the area for $\tan \beta = 44$ originates from the CDM



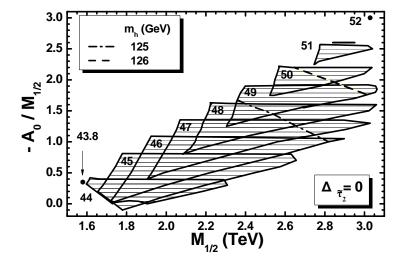


Fig. 8. Allowed regions in the $M_{1/2}-A_0/M_{1/2}$ plane for $\Delta_{\tilde{\tau}_2}=0$ and various $\tan\beta$'s indicated in the graph. The dot-dashed [dashed] line corresponds to $m_h=125~[126]~{\rm GeV}$.

bound in Eq. (55). The dot-dashed and dashed lines correspond to $m_h=125$ and $126~{\rm GeV}$ respectively. We see that the m_h 's which are favored by LHC can be readily obtained in our model for the higher allowed values of $\tan \beta$.

The overall allowed parameter space can be designed in the $tan\beta - A_0/M_{1/2}$ plane as shown in Fig. 9. Each point in the shaded space of this figure corresponds to an allowed area in the $M_{1/2} - m_0$ plane similar to the thin strips shown in Fig. 7. The lower boundary of the allowed parameter space in Fig. 9 originates from the limit on BR $(B_s \to \mu^+ \mu^-)$ in Eq. (48), except its leftmost part which comes from the lower bound on m_h in Eq. (47) or the CDM bound in Eq. (55). The upper boundary comes from the CDM bound in Eq. (55). We see that $\tan \beta$ ranges from about 43.8 to 52. These values are only a little smaller than the ones obtained in the case of exact YU or the monoparametric YQUCs discussed in Refs. 35, 37–39, 41, 42. This mild reduction of $\tan \beta$ is, however, adequate to reduce the extracted BR $(B_s \to \mu^+\mu^-)$ to an acceptable level compatible with the CDM requirement. In the allowed area of Fig. 9, the parameter $A_0/M_{1/2}$ ranges from about -3 to 0.1. We also find that, in this allowed area, the Higgs mass m_h ranges from 122 to 127.23 GeV and the LSP mass $m_{\rm LSP}$ from about 746.5 to 1433 GeV. So we see that, although m_h 's favored by LHC can be easily accommodated, the lightest neutralino mass is large making its direct detection very difficult. At the maximum allowed $m_{\rm LSP}$, BR $(B_s \to \mu^+ \mu^-)$ takes its minimal value in the allowed parameter space. This value turns out to be about $3.64 \times$ 10^{-9} and, thus, the lower bound in Eq. (49) is satisfied everywhere in the allowed area in Fig. 9. The range of the discrepancy δa_{μ} between the measured muon anomalous magnetic moment and its SM value in the allowed parameter space of Fig. 9 is about $(0.35 - 2.76) \times$ 10^{-10} (note that δa_{μ} decreases as $\tan \beta$ or $M_{1/2}$ increases). Therefore, Eq. (52) is satisfied only at the level of 2.55 to $2.82-\sigma$. Note that, had we considered the $\mu<0$ case, δa_{μ}

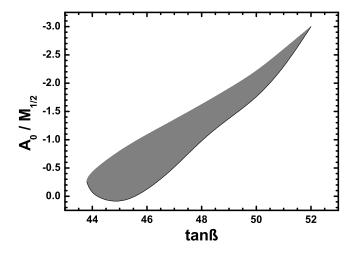


Fig. 9. The overall (shaded) allowed parameter space of the model in the $tan\beta - A_0/M_{1/2}$ plane.

would have been negative and the violation of Eq. (52) would have certainly been stronger than for $\mu > 0$.

In Table 2, we list the input and the output parameters of the present model, the masses in TeV of the SUSY particles (gauginos/higgsinos $\tilde{\chi},~\tilde{\chi}_2^0,~\tilde{\chi}_3^0,~\tilde{\chi}_4^0,~\tilde{\chi}_1^\pm,~\tilde{\chi}_2^\pm,~\tilde{g}$, squarks $\tilde{t}_1,\ \tilde{t}_2,\ \tilde{b}_1,\ \tilde{b}_2,\ \tilde{u}_L,\ \tilde{u}_R,\ \tilde{d}_L,\ \tilde{d}_R,$ and sleptons $\tilde{ au}_1,\ \tilde{ au}_2,\ \tilde{
u}_{ au},\ \tilde{
u}_e,\ \tilde{e}_L,\ \tilde{e}_R)$ and the Higgses (h, H, H^{\pm}, A) , and the values of the various low energy observables in four characteristic cases (recall that 1 pb $\simeq 2.6 \times 10^{-9} \text{ GeV}^{-2}$). Note that we have considered the squarks and sleptons of the two first generations as degenerate. From the values of the various observable quantities, it is easy to verify that all the relevant constraints are met. In the low energy observables, we included the spin-independent (SI) and spin-dependent (SD) lightest neutralino-proton $(\tilde{\chi}p)$ scattering cross sections $\sigma_{\tilde{\chi}p}^{\rm SI}$ and $\sigma_{\tilde{\chi}p}^{\rm SD}$, respectively, using central values for the hadronic inputs – for the details of the calculation, see Ref. 39. We see that, these cross sections are well below not only the present experimental upper bounds, but even the projected sensitivity of all planned future experiments. So, the allowed parameter space of our model will not be accessible to the planned CDM direct detection experiments based on neutralino-proton scattering. We also notice that, the sparticles turn out to be very heavy, which makes their discovery a very difficult task.

The fact that, in our model, $M_{1/2}$, m_0 , and μ generally turn out to be of the order of a few TeV puts under some stress the naturalness of the radiative EWSB – see Eq. (37). This is, though, a general problem of the CMSSM, especially in view of the recent data on $B_s \to \mu^+\mu^-$ and m_h as noted in Ref. 131–133. Attempts to address this problem, known as little hierarchy problem, invoke departures from the CMSSM universality^{158–162} or addition of extra matter superfields 163 - singlet 25-27 or vector-like 164-166 - beyond the MSSM ones.

Table 2. Input/output parameters, sparticle and Higgs masses, and low energy observables in four cases.

Input Parameters									
$\tan \beta$	48	49	50	51					
$-A_0/M_{1/2}$	1.4	1.6	2	2.5					
$M_{1/2}/\text{TeV}$	2.27	2.411	2.824	2.808					
$m_0/{ m TeV}$	1.92	2.295	3.156	3.747					
Output Parameters									
$h_t/h_{ au}(M_{ m GUT})$	1.117	1.079	1.038	1.008					
$h_b/h_{ au}(M_{ m GUT})$	0.623	0.618	0.613	0.607					
$h_t/h_b(M_{ m GUT})$	1.792	1.745	1.693	1.660					
$\mu/{ m TeV}$	2.78	3.092	3.823	4.129					
$\Delta_{ ilde{ au}_2}(\%)$	1.43	0.93	0.1	0.17					
$\Delta_H(\%)$	3.08	1.30	0.11	1.76					
Masses in TeV of Sparticles and Higgses									
$ ilde{\chi}, ilde{\chi}_2^0$	1.023, 1.952	1.110, 2.117	1.309, 2.489	1.303, 2.481					
$ ilde{\chi}^0_3, ilde{\chi}^0_4$	2.782, 2.785	3.088, 3.091	3.815, 3.817	4.114, 4.116					
$ ilde{\chi}_1^{\pm}, ilde{\chi}_2^{\pm}$	1.985, 2.785	2.117, 3.091	2.489, 3.817	2.481, 4.116					
$ ilde{ ilde{g}} ilde{ ilde{t}}_1, ilde{t}_2$	4.809	5.190	6.042	6.040					
$ ilde{t}_1, ilde{t}_2$	3.806, 3.226	4.097, 3.458	4.761, 3.967	4.781, 3.902					
$ ilde{b}_1, ilde{b}_2$	3.838, 3.763	4.141, 4.058	4.853, 4.733	4.947, 4.757					
$ ilde{u}_L, ilde{u}_R$	4.687, 4.485	5.138, 4.923	6.186, 5.946	6.483, 6.257					
$ ilde{d}_L, ilde{d}_R$	4.687, 4.459	5.138, 4.896	6.187, 5.914	6.483, 6.227					
$ ilde{ au}_1, ilde{ au}_2$	2.082, 1.037	2.347, 1.121	2.979, 1.310	3.293, 1.305					
$ ilde{ u}_{ au}, ilde{ u}_{e}$	2.075, 2.451	2.342, 2.818	2.975, 3.689	3.289, 4.200					
$ ilde{e}_L, ilde{e}_R$	2.453, 2.112	2.819, 2.476	3.690, 3.339	4.201, 3.901					
h, H	0.1245, 2.109	0.125, 2.249	0.126, 2.621	0.1265, 2.652					
H^{\pm}, A	2.111, 2.110	2.251, 2.25	2.623, 2.622	2.654, 2.652					
Low Energy Observables									
$10^4 \mathrm{BR} \left(b \to s \gamma \right)$	3.25	3.25	3.26	3.26					
$10^9 \mathrm{BR} \left(B_s \to \mu^+ \mu^- \right)$	4.17	4.15	3.98	4.17					
$R\left(B_u \to \tau \nu\right)$	0.975	0.977	0.982	0.982					
$10^{10}\delta a_{\mu}$	1.11	0.89	0.57	0.49					
$\Omega_{\mathrm{LSP}} h^2$	0.11	0.11	0.11	0.11					
$\sigma_{\tilde{\chi}p}^{\rm SI}/10^{-12} { m pb}$	6.17	4.55	2.44	1.75					
$\sigma_{\tilde{\chi}p}^{SD}/10^{-9} \text{pb}$	1.69	1.08	0.43	0.28					

7. The Deviation from Yukawa Unification

In the overall allowed parameter space of our model in Fig. 9, we find the following ranges for the ratios of the asymptotic third generation Yukawa coupling constants: $h_t/h_\tau \simeq 0.98-1.29, h_b/h_\tau \simeq 0.60-0.65$, and $h_t/h_b \simeq 1.62-2.00$. We observe that, although exact YU is broken, these ratios remain close to unity. They can generally be obtained by natural values of the real and positive parameter ρ and the complex parameters

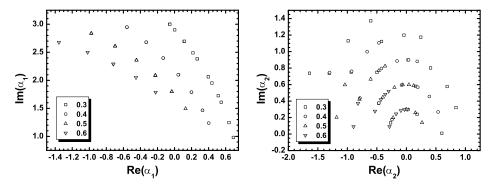


Fig. 10. The complex parameters α_1 and α_2 for various values of the real and positive parameter ρ , which are indicated in the graphs, for the case presented in the second column of Table 2 with $tan\beta=49$ and $m_h=60$ $125~{\rm GeV}$.

 α_1 , α_2 , which enter the YQUCs in Eq. (23). Comparing these ratios with the ones of the gauge coupling constants of the non-SUSY SM at a scale close to $M_{\rm GUT}$ – see e.g. Ref. 98 -, we can infer that the ratios here are not as close to unity. Despite this fact, we still apply the term 'Yukawa quasi-unification' in the sense that the ratios of the Yukawa coupling constants in our model are much closer to unity than in generic models with lower values of $\tan \beta$ – cf. Ref. 167, 168. Finally, note that the deviation from exact YU here is comparable to the one obtained in the monoparametric case – cf. Ref. 39 – and is also generated in a natural, systematic, controlled, and well-motivated manner.

In order to see that these ratios can be obtained by natural values of ρ , α_1 , and α_2 , we take as a characteristic example the second out of the four cases presented in Table 2, which yields $m_h = 125 \text{ GeV}$ favored by the LHC. In this case, where $h_b/h_\tau = 0.618$ and $h_t/h_\tau=1.079$, we solve Eq. (23) w.r.t. the complex parameters α_1 , α_2 for various values of the real and positive parameter ρ . Needless to say that one can find infinitely many solutions, since we have only two equations and five real unknowns. Some of these solutions are shown Fig. 10. Note that the equation for h_b/h_τ depends only on the combination $\rho\alpha_1$ and, therefore, its solutions are expected to lie on a certain curve in the complex plane of this combination. Consequently, in the α_1 complex plane, the solutions should be distributed on a set of similar curves corresponding to the various values of the real and positive parameter ρ . This is indeed the case as one can see from the left panel of Fig. 10. For each α_1 and ρ in this panel, we then solve the equation for h_t/h_τ to find the complex parameter α_2 . In the right panel of Fig. 10, we show several such solutions. Observe that the equation for h_t/h_τ depends separately on α_2 and ρ and, thus, its solutions do not follow any specific pattern in the α_2 complex plane. Note that each point in the α_1 complex plane generally corresponds to more than one points in the α_2 complex plane. We scanned the range of ρ from 0.3 to 3 and found solutions only for the lower values of this parameter (up to about 0.6). The solutions found for α_1 and α_2 are also limited in certain natural regions of the corresponding complex planes. The picture is very similar to the one just described for all the possible values of the ratios of the third generation Yukawa coupling constants

encountered in our investigation. So, we conclude that these ratios can be readily obtained by a multitude of natural choices of the parameters ρ , α_1 , and α_2 everywhere in the overall allowed parameter space of the model.

8. The Hyperbolic Branch/Focus Point Area

It is generally accepted that the mSUGRA/CMSSM parameter space has been significantly squeezed by the recent experimental results. In particular, in most of the allowed parameter space, the LSP and the other sparticles turn out to be too heavy and a mild tuning is required for achieving the radiative EWSB. As discussed above, the CMSSM with (generalized) Yukawa quasi-unification is not an exception at least in the H-pole enhanced stau-antistau coannihilation regime considered here. There exists, though, a broader viable region of the parameter space of the CMSSM, which does not require excessive electroweak fine tuning and can yield a relatively light LSP. This region, which is characterized by large values of the ratio $m_0/M_{1/2}$, is known as the HB/FP regime. $^{150-156}$

In our model, we also find a viable HB/FP area with the LSP still being the lightest neutralino, but now with a significant higgsino component. Its mass can even be well below 100 GeV. This area extends to large m_0 's (> 15 TeV) and $M_{1/2}$'s, but its most interesting part is the one at low $M_{1/2}$'s. In this part and for small m_0 's, the reduction of $\Omega_{\rm LSP}h^2$ is mostly caused by $\tilde{\chi}\tilde{\chi}$ annihilation effects. As m_0 gets larger, the neuralino-chargino and chargino-chargino coannihilation effects become dominant. The constraints from B physics are all well satisfied in this regime. On the other hand, the value of δa_μ is still below the lower bound in Eq. (53). The ratios of the third generation Yukawa coupling constants remain close to unity. Having in mind the latest indications for a light candidate CDM particle from the CDMS II experiment, ¹⁶⁹ we see that the HB/FP region is very promising and it definitely needs more light to be shed on it. We are currently pursuing the detailed investigation of this region.

9. Conclusions

We performed an analysis of the parameter space of the CMSSM with $\mu>0$ supplemented by a generalized asymptotic Yukawa coupling quasi-unification condition, which is implied by the SUSY GUT constructed in Ref. 35 and allows an experimentally acceptable b-quark mass. We imposed a number of cosmological and phenomenological constraints originating from the CDM abundance in the universe, B physics ($b \to s\gamma$, $B_s \to \mu^+\mu^-$, and $B_u \to \tau\nu$), and the mass m_h of the lightest neutral CP-even Higgs boson. We found that the lightest neutralino can act as a CDM candidate in a relatively wide range of parameters. In particular, the upper bound from CDM considerations on the lightest neutralino relic abundance, which is drastically reduced mainly by H-pole enhanced stau-antistau coannihilation processes, is compatible with the recent data on the branching ratio of $B_s \to \mu^+\mu^-$ in this range of parameters. Also, values of $m_h \simeq (125-126)~{\rm GeV}$, which are favored by the LHC, can be easily accommodated. The mass of the lightest neutralino, though, comes out to be large ($\sim 1~{\rm TeV}$), which makes its direct detectability very difficult and the sparticle spectrum very heavy.

Acknowledgments

This work was supported by the European Union under the Marie Curie Initial Training Network 'UNILHC' PITN-GA-2009-237920 and the Greek Ministry of Education, Lifelong Learning, and Religious Affairs and the Operational Program: Education and Lifelong Learning 'HERACLITOS II'.

References

- 1. A.H. Chamseddine, R.L. Arnowitt, and P. Nath, Phys. Rev. Lett. 49, 970 (1982).
- 2. P. Nath, R.L. Arnowitt, and A.H. Chamseddine, Nucl. Phys. B227, 121 (1983).
- 3. N. Ohta, *Prog. Theor. Phys.* **70**, 542 (1983).
- 4. L.J. Hall, J.D. Lykken, and S. Weinberg, *Phys. Rev. D* 27, 2359 (1983).
- R. Arnowitt, A. H. Chamseddine, And Pran Nath, Int. J. Mod. Phys. A 27, 1230028 (2012).
- 6. R.L. Arnowitt and P. Nath, *Phys. Rev. Lett.* **69**, 725 (1992).
- 7. G.G. Ross and R.G. Roberts, *Nucl. Phys.* **B377**, 571 (1992).
- 8. V.D. Barger, M.S. Berger, and P. Ohmann, Phys. Rev. D 49, 4908 (1994).
- 9. G.L. Kane, C. Kolda, L. Roszkowski, and J.D. Wells, *Phys. Rev. D* 49, 6173 (1994).
- 10. G. Lazarides and C. Panagiotakopoulos, Phys. Lett. B 337, 90 (1994).
- 11. S. Khalil, G. Lazarides, and C. Pallis, Phys. Lett. B 508, 327 (2001).
- 12. B. Ananthanarayan, G. Lazarides, and Q. Shafi, Phys. Rev. D 44, 1613 (1991).
- 13. B. Ananthanarayan, G. Lazarides, and Q. Shafi, Phys. Lett. B 300, 245 (1993).
- 14. T. Blažek, R. Dermíšek, and S. Raby, Phys. Rev. Lett. 88, 111804 (2002).
- 15. T. Blažek, R. Dermíšek, and S. Raby, *Phys. Rev. D* **65**, 115004 (2002).
- 16. R. Dermíšek, S. Raby, L. Roszkowski, and R. Ruiz de Austri, J. High Energy Phys. **04**, 037 (2003).
- 17. M.S. Carena, M. Olechowski, S. Pokorski, and C.E.M. Wagner, Nucl. Phys. B426, 269 (1994).
- 18. R. Hempfling, *Phys. Rev. D* **49**, 6168 (1994).
- 19. L.J. Hall, R. Rattazzi, and U. Sarid, *Phys. Rev. D* **50**, 7048 (1994).
- 20. M. Davier, A. Hoecker, B. Malaescu, and Z. Zhang, Eur. Phys. J. C 71, 1515 (2011); 72, 1874(E)
- 21. K. Hagiwara, R. Liao, A.D. Martin, D. Nomura, and T. Teubner, J. Phys. G 38, 085003 (2011).
- 22. T. Aoyama, M. Hayakawa, T. Kinoshita, and M. Nio, Phys. Rev. Lett. 109, 111808 (2012).
- 23. F. Jegerlehner and R. Szafron, Eur. Phys. J. C 71, 1632 (2011).
- 24. M. Benayoun, P. David, L. DelBuono, and F. Jegerlehner, Eur. Phys. J. C 72, 1848 (2012).
- 25. S.F. King, M. Muhlleitner, and R. Nevzorov, Nucl. Phys. **B860**, 207 (2012).
- 26. J.F. Gunion, Y. Jiang, and S. Kraml, Phys. Lett. B 710, 454 (2012).
- 27. K.J. Bae, K. Choi, E.J. Chun, S.H. Im, C.B. Park, and C.S. Shin, arXiv:1208.2555.
- 28. H. Baer, M.A. Diaz, J. Ferrandis, and X. Tata, Phys. Rev. D 61, 111701 (2000).
- 29. H. Baer, M. Brhlik, M.A. Diaz, J. Ferrandis, P. Mercadante, P. Quintana, and X. Tata, Phys. Rev. *D* **63**, 015007 (2000).
- 30. D. Auto, H. Baer, C. Balázs, A. Belyaev, J. Ferrandis, and X. Tata, J. High Energy Phys. **06**, 023 (2003).
- 31. D. Auto, H. Baer, A. Belyaev, and T. Krupovnickas, J. High Energy Phys. 10, 066 (2004).
- 32. U. Chattopadhyay and P. Nath, Phys. Rev. D 65, 075009 (2002).
- 33. U. Chattopadhyay, A. Corsetti, and P. Nath, Phys. Rev. D 66, 035003 (2002).
- 34. C. Pallis, Nucl. Phys. B678, 398 (2004).
- 35. M.E. Gómez, G. Lazarides, and C. Pallis, Nucl. Phys. B638, 165 (2002).
- 36. M.E. Gómez, G. Lazarides, and C. Pallis, Phys. Rev. D 67, 097701 (2003).
- 37. G. Lazarides and C. Pallis, hep-ph/0404266.

- 38. G. Lazarides and C. Pallis, hep-ph/0406081.
- 39. N. Karagiannakis, G. Lazarides, and C. Pallis, Phys. Lett. B 704, 43 (2011).
- 40. S. Dar, I. Gogoladze, Q. Shafi, and C.S. Un, Phys. Rev. D 84, 085015 (2011).
- 41. N. Karagiannakis, G. Lazarides, and C. Pallis, PoS (CORFU2011), 023 (2012).
- 42. N. Karagiannakis, G. Lazarides, and C. Pallis, J. Phys. Conf. Ser. 384, 012012 (2012).
- 43. S.F. King and M. Oliveira, *Phys. Rev. D* **63**, 015010 (2001).
- 44. I. Gogoladze, R. Khalid, and Q. Shafi, Phys. Rev. D 79, 115004 (2009).
- 45. I. Gogoladze, R. Khalid, and Q. Shafi, Phys. Rev. D 80, 095016 (2009).
- 46. I. Gogoladze, R. Khalid, S. Raza, and Q. Shafi, J. High Energy Phys. 12, 055 (2010).
- 47. I. Antoniadis and G.K. Leontaris, Phys. Lett. B 216, 333 (1989).
- 48. R. Jeannerot, S. Khalil, G. Lazarides, and Q. Shafi, J. High Energy Phys. 10, 012 (2000).
- 49. G. Lazarides, Q. Shafi, and C. Wetterich, Nucl. Phys. **B181**, 287 (1981).
- 50. G. Lazarides and Q. Shafi, Nucl. Phys. B350, 179 (1991).
- 51. R. Jeannerot, S. Khalil, and G. Lazarides, J. High Energy Phys. 07, 069 (2002).
- 52. G. Lazarides and A. Vamvasakis, Phys. Rev. D 76, 083507 (2007)
- 53. G. Lazarides and A. Vamvasakis, Phys. Rev. D 76, 123514 (2007).
- 54. G. Lazarides, I.N.R. Peddie, and A. Vamvasakis, Phys. Rev. D 78, 043518 (2008).
- 55. G. Lazarides, arXiv:1006.3636.
- 56. G.'t Hooft, Nucl. Phys. B79, 276 (1974).
- 57. A.M. Polyakov, JETP Lett. 20, 194 (1974).
- 58. J.P. Preskill, Phys. Rev. Lett. 43, 1365 (1979).
- 59. G. Lazarides, Q. Shafi, and W.P. Trower, Phys. Rev. Lett. 49, 1756 (1982).
- 60. G. Lazarides and Q. Shafi, Phys. Lett. B 258, 305 (1991).
- 61. G. Lazarides, Q. Shafi, and N.D. Vlachos, Phys. Lett. B 427, 53 (1998).
- 62. G. Aad et al. [ATLAS Collaboration], Phys. Lett. B 716, 1 (2012).
- 63. S. Chatrchyan et al. [CMS Collaboration], Phys. Lett. B 716, 30 (2012).
- 64. T. Aaltonen et al. [CDF and D0 Collaborations], Phys. Rev. Lett. 109, 071804 (2012).
- 65. R. Aaij et al. [LHCb Collaboration], Phys. Rev. Lett. 108, 231801 (2012).
- 66. J. Albrecht, Mod. Phys. Lett. A 27, 1230028 (2012).

The ATLAS, CMS, and LHCb Collaborations,

- 67. E. Komatsu *et al.* [WMAP Collaboration], *Astrophys. J. Suppl.* **192**, 18 (2011). http://lambda.gsfc.nasa.gov/product/map.
- http://cds.cern.ch/record/1452186/files/LHCb-CONF-2012-017.pdf. 69. N. Karagiannakis, G. Lazarides, and C. Pallis, *Phys. Rev. D* 87, 055001 (2013).
- 70. C. Pallis and N. Toumbas, *J. Cosmol. Astropart. Phys.* **12**, 002 (2011).
- 71. R. Peccei and H. Quinn, *Phys. Rev. Lett.* **38**, 1440 (1977).
- 71. R. Peccei and H. Quilli, *Phys. Rev. Lett.* **36**, 144
- 72. S. Weinberg, Phys. Rev. Lett. 40, 223 (1978).
- 73. F. Wilczek, *Phys. Rev. Lett.* **40**, 279 (1978).
- 74. G. Lazarides, C. Panagiotakopoulos, and Q. Shafi, Phys. Rev. Lett. 56, 432 (1986).
- 75. N. Ganoulis, G. Lazarides, and Q. Shafi, Nucl. Phys. B323, 374 (1989).
- 76. G. Lazarides and Q. Shafi, Nucl. Phys. **B329**, 182 (1990).
- 77. G. Lazarides and Q. Shafi, Phys. Rev. D 58, 071702 (1998).
- 78. J.E. Kim and H.P. Nilles, Phys. Lett. B 138, 150 (1984).
- 79. H. Murayama, H. Suzuki, and T. Yanagida, Phys. Lett. B 291, 418 (1992).
- 80. K. Choi, E.J. Chun, and J.E. Kim, Phys. Lett. B 403, 209 (1997).
- 81. G. Lazarides and Q. Shafi, Phys. Lett. B 489, 194 (2000).
- 82. E.J. Chun, K. Dimopoulos and D. Lyth, Phys. Rev. D 70, 103510 (2004).
- 83. A. Anisimov and M. Dine, J. Cosmol. Astropart. Phys. 07, 009 (2005).
- 84. L. Dolan and R. Jackiw, Phys. Rev. D 9, 3320 (1974).
- 85. S. Weinberg, Phys. Rev. D 9, 3357 (1974).

- 86. K. Dimopoulos, G. Lazarides, D. Lyth, and R. Ruiz de Austri, J. High Energy Phys. 05, 057 (2003).
- 87. K. Kadota and K. A. Olive, Phys. Rev. D 80, 095015 (2009).
- 88. J.R. Ellis, K.A. Olive, Y. Santoso, and V.C. Spanos, Phys. Rev. D 70, 055005 (2004).
- 89. E. Dudas, Y. Mambrini, A. Mustafayev, and K.A. Olive, Eur. Phys. J. C 72, 2138 (2012).
- 90. D.M. Pierce, J.A. Bagger, K.T. Matchev, and R. Zhang, *Nucl. Phys.* **B491**, 3 (1997).
- 91. M.S. Carena, D. Garcia, U. Nierste, and C.E.M. Wagner, Nucl. Phys. B577, 88 (2000).
- 92. M. Drees and M.M. Nojiri, *Phys. Rev. D* **45**, 2482 (1992).
- 93. H. Baer, C. Chen, M. Drees, F. Paige, and X. Tata, Phys. Rev. Lett. 79, 986 (1997).
- 94. B.C. Allanach, Comput. Physics Commun. 143, 305 (2002).
- 95. P.Z. Skands et al., J. High Energy Phys. 07, 036 (2004).
- 96. M.E. Gómez, G. Lazarides, and C. Pallis, Phys. Rev. D 61, 123512 (2000).
- 97. M.E. Gómez, G. Lazarides, and C. Pallis, Phys. Lett. B 487, 313 (2000).
- 98. H. Baer and X. Tata, Weak Scale Supersymmetry: From Superfields to Scattering Events (Cambridge University Press, Cambridge, UK, 2006).
- 99. K. Nakamura et al. [Particle Data Group], J. Phys. G 37, 075021 (2010).
- 100. H. Baer, J. Ferrandis, K. Melnikov, and X. Tata, Phys. Rev. D 66, 074007 (2002).
- 101. K. Tobe and J.D. Wells, Nucl. Phys. **B663**, 123 (2003).
- 102. Tevatron Electroweak Working Group [CDF and D0 Collaborations], arXiv:0903.2503.
- 103. T. Aaltonen et al. [CDF Collaboration], Phys. Rev. Lett. 105, 252001 (2010).
- 104. G. Belanger, F. Boudjema, A. Pukhov, and A. Semenov, http://lapth.in2p3.fr/micromegas.
- 105. G. Belanger, F. Boudjema, P. Brun, A. Pukhov, S. Rosier-Lees, P. Salati, and A. Semenov, Comput. Phys. Commun. 182, 842 (2011).
- 106. G. Degrassi, P. Slavich, and F. Zwirner, Nucl. Phys. **B611**, 403 (2001).
- 107. A. Brignole, G. Degrassi, P. Slavich, and F. Zwirner, Nucl. Phys. B6312002195.
- 108. A. Brignole, G. Degrassi, P. Slavich, and F. Zwirner, Nucl. Phys. B643, 79 (2002).
- 109. A. Dedes, G. Degrassi, and P. Slavich, Nucl. Phys. B6722003144.
- 110. B.C. Allanach, S. Kraml, and W. Porod, J. High Energy Phys. 03, 045 (2003).
- 111. B.C. Allanach, A. Djouadi, J.L. Kneur, W. Porod, and P. Slavich, J. High Energy Phys. 09, 044 (2004).
- 112. P.H. Chankowski and L. Slawianowska, Phys. Rev. D 63, 054012 (2001).
- 113. C.S. Huang, W. Liao, Q.S. Yan, and S.H. Zhu, Phys. Rev. D 63, 114021 (2001); 64, 059902(E)
- 114. C. Bobeth, T. Ewerth, F. Kruger, and J. Urban, *Phys. Rev. D* **64**, 074014 (2001).
- 115. A. Dedes, H.K. Dreiner, and U. Nierste, Phys. Rev. Lett. 87, 251804 (2001).
- 116. J.R. Ellis, K.A. Olive, and V.C. Spanos, Phys. Lett. B 624, 47 (2005).
- 117. F. Mahmoudi, Comput. Phys. Commun. 180, 1579 (2009).
- 118. The CMS and LHCb Collaborations,
 - http://cdsweb.cern.ch/record/1374913/files/BPH-11-019-pas.pdf.
- 119. R. Aaij et al. [LHCb Collaboration], Phys. Rev. Lett. 110, 021801 (2013).
- 120. E. Barberio et al. [Heavy Flavor Averaging Group], arXiv:0808.1297.
- 121. M. Misiak et al., Phys. Rev. Lett. 98, 022002 (2007).
- 122. G. Bélanger, F. Boudjema, A. Pukhov, and A. Semenov, Comput. Phys. Commun. 174, 577
- 123. M. Ciuchini, G. Degrassi, P. Gambino, and G.F. Giudice, Nucl. Phys. B527, 21 (1998).
- 124. F. Borzumati and C. Greub, Phys. Rev. D 58, 074004 (1998).
- 125. G. Degrassi, P. Gambino, and G.F. Giudice, J. High Energy Phys. 12, 009 (2000).
- 126. M.E. Gómez, T. Ibrahim, P. Nath, and S. Skadhauge, Phys. Rev. D 74, 015015 (2006).
- 127. G. Isidori and P. Paradisi, Phys. Lett. B 639, 499 (2006).

- 128. G. Isidori, F. Mescia, P. Paradisi, and D. Temes, Phys. Rev. D 75, 115019 (2007).
- 129. S.P. Martin and J.D. Wells, *Phys. Rev. D* **64**, 035003 (2001).
- 130. G.W. Bennett *et al.* [Muon g 2 Collaboration], *Phys. Rev. D* **73**, 072003 (2006).
- 131. J. Ellis and K.A. Olive, Eur. Phys. J. C 72, 2005 (2012).
- 132. A. Fowlie et al., Phys. Rev. D 86, 075010 (2012).
- 133. O. Buchmueller et al., Eur. Phys. J. C 72, 2243 (2012).
- 134. P.A.R. Ade et al. [Planck Collaboration], arXiv:1303.5076.
- 135. C. Pallis, Astropart. Phys. 21, 689 (2004).
- 136. C. Pallis, J. Cosmol. Astropart. Phys. 10, 015 (2005).
- 137. C. Pallis, Nucl. Phys. B751, 129 (2006).
- 138. C. Pallis, hep-ph/0610433.
- 139. L. Covi, L. Roszkowski, R. Ruiz de Austri, and M. Small, J. High Energy Phys. 06, 003 (2004).
- 140. K.-Y. Choi, L. Covi, J.E. Kim, and L. Roszkowski, J. High Energy Phys. 04, 106 (2012).
- 141. H. Baer and H. Summy, Phys. Lett. B 666, 5 (2008).
- 142. H. Baer, M. Haider, S. Kraml, S. Sekmen, and H. Summy, *J. Cosmol. Astropart. Phys.* **02**, 002 (2009).
- 143. H. Baer, A.D. Box, and H. Summy, J. High Energy Phys. 10, 023 (2010).
- 144. J.R. Ellis, T. Falk, and K.A. Olive, *Phys. Lett. B* **444**, 367 (1998).
- J.R. Ellis, T. Falk, K.A. Olive, and M. Srednicki, Astropart. Phys. 13, 181 (2000); 15, 413(E) (2001).
- 146. A.B. Lahanas, D.V. Nanopoulos, and V.C. Spanos, *Phys. Rev. D* **62**, 023515 (2000).
- 147. J.R. Ellis, T. Falk, G. Ganis, K.A. Olive, and M. Srednicki, Phys. Lett. B 510, 236 (2001).
- 148. T. Nihei, L. Roszkowski, and R. Ruiz de Austri, J. High Energy Phys. 05, 063 (2001).
- 149. T. Nihei, L. Roszkowski, and R. Ruiz de Austri, J. High Energy Phys. 07, 024 (2002).
- 150. H. Baer, C.H. Chen, C. Kao, and X. Tata, Phys. Rev. D 52, 1565 (1995).
- 151. K.L. Chan, U. Chattopadhyay, and P. Nath, Phys. Rev. D 58, 096004 (1998).
- 152. J. Feng, K. Matchev, and T. Moroi, Phys. Rev. Lett. 84, 2322 (2000).
- 153. J. Feng, K. Matchev, and T. Moroi, Phys. Rev. D 61, 075005 (2000).
- 154. J.L. Feng, K.T. Matchev, and D. Sanford, Phys. Rev. D 85, 075007 (2012).
- 155. H. Baer, V. Barger, and A. Mustafayev, J. High Energy Phys. 05, 091 (2012).
- 156. V.E. Mayes, Int. J. Mod. Phys. A 28, 1350061 (2013).
- 157. J. Ellis, K. Olive and Y. Santoso, *Astropart. Phys.* 18, 395 (2003).
- 158. J. Ellis, F. Luo, K. A. Olive, and P. Sandick, arXiv:1212.4476.
- 159. H. Baer, V. Barger, P. Huang, A. Mustafayev, and X. Tata, Phys. Rev. Lett. 109, 161802 (2012).
- 160. H. Baer, S. Kraml, and S. Kulkarni, J. High Energy Phys. 12, 066 (2012).
- 161. H. Baer, V. Barger, P. Huang, D. Mickelson, A. Mustafayev, and X. Tata, arXiv:1212.2655.
- 162. I. Gogoladze, F. Nasir, and Q. Shafi, Int. J. Mod. Phys. A 28, 1350046 (2013).
- 163. L. Hall, D. Pinner, and J. Ruderman, J. High Energy Phys. **04**, 131 (2012).
- 164. S.P. Martin, Phys. Rev. D 81, 035004 (2010).
- 165. S.P. Martin, Phys. Rev. D 82, 055019 (2010).
- 166. K.J. Bae, T.H. Jung, and H.D. Kim, Phys. Rev. D 87, 015014 (2013).
- S. Antusch, L. Calibbi, V. Maurer, M. Monaco, and M. Spinrath, *Phys. Rev. D* 85, 035025 (2012).
- 168. S. Antusch, L. Calibbi, V. Maurer, M. Monaco, and M. Spinrath, *J. High Energy Phys.* **01**, 187 (2013).
- 169. R. Agnese et al. [CDMS Collaboration], arXiv:1304.4279.